STUDY OF CROSS-ROLLED GRAIN-ORIENTED Fe - Si ALLOYS

BY

J. V. KUMAR

DEPARTMENT OF METALLURGICAL ENGINEERING

INDIAN INSTITUTE OF TECHNOLOGY KANPUR

MARCH 1972

STUDY OF CROSS-ROLLED GRAIN-ORIENTED
Fe - Si ALLOYS

A Thesis Submitted
In Partial Fulfilment of the Requirements
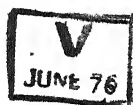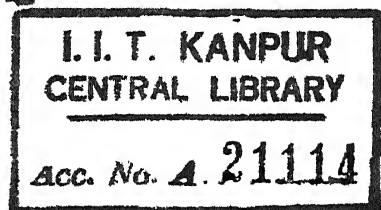for the Degree of
MASTER OF TECHNOLOGY

BY

J. V. KUMAR

to the

DEPARTMENT OF METALLURGICAL ENGINEERING
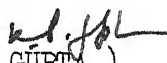# INDIAN INSTITUTE OF TECHNOLOGY KANPUR
MARCH 1972

ME-1972-M-KUM-STU

<u>CERTIFICATE</u>

This is to certify that this work on " Study of Cross-Rolled Grain-Oriented Fe-Si Alloys" has been carried out under my supervision and it has not been submitted elsewhere for a degree.

(K.P. GUPTA)
Professor and Head
Department of Metallurgical Engineering
Indian Institute of Technology , Kanpur

ACKNOWLEDGEMENTS

CONTENTS

SYNOPSIS

The cold rolled texture of iron silicon alloys (b.c.c.) is basically (100) $[01\bar{1}]$ texture, usually with deviations from the ideal texture. If the texture is perfected, the sheets have two $[\bar{1}00]$ directions (the directions of easy magnetisation) at 45° to the rolling direction lying on the rolling plane, so that the textured sheets cut at 45° to the rolling direction can be used in transformer cores. The power losses will be minimised by using such steel sheets.

Cross rolling is shown to sharpen the cold rolled texture. The effects of unequal amounts of cross rolling and low temperature annealings of the cross rolled products are presented.

I. INTRODUCTION

INTRODUCTION

Single crystals of magnetic materials are anisotropic; that is, they have different magnetic properties in different crystallographic directions. Kaya & Honda[1] showed that a single crystal of iron can be magnetized more easily in the [001] direction than in the [110] and [111] directions (Figs. 1 and 3); the [111] direction being the hardest direction to magnetize. The same observations were made by Williams[2] for the Fe-Si alloys, (Fig.2).

The metal or alloy in bulk form behaves isotropically because of randomly oriented grain structure. In polycrystalline material, if the grains are oriented with their easy directions of magnetization in the same direction, better magnetic behaviour is expected. The three principal applications of this idea are the directional-grain ALNICO permanent magnets, the oriented 50-50% Fe- Ni alloys which are used in magnetic amplifiers and the grain-oriented Si-Fe alloys, used in power transformers.

Fe-Si alloys are superior to pure Fe in their magnetic properties[2,3]. Addition of Si to Fe is advantageous for a number of reasons, the most important of which are increased electrical resistivity (leading to lower eddy current losses) (Fig. 4), reduction in hysteresis losses (Fig.5), increased maximum permeability which rapidly increases beyond about 3% Si and reaches a maximum at 6% Si (Fig. 4). For magnetic steel the saturation intensity of magnetization, permeability and resistivity must be high. Hence a proper amount of Si in Fe is required to produce the desired material. However, if Si-content increases beyond about 5%, the material becomes brittle (Fig. 6). Hence, all commercial alloys normally

contain less than 5% Si, usually upto about 4.5% Si. The amount
of Si depends on the magnetic properties required in the material.
Other impurities affect the magnetic properties of iron (Fig. 7).
Carbon, which is the most common of all impurities, increases the
hysteresis losses at a very rapid rate up to 0.01%. Sulphur and
oxygen also increase the hysteresis losses, but the rate of
increase is smaller than that produced by carbon additions. Mn
does not have appreciable effect on losses. Phosphorous decreases
the hysteresis losses. To some extent phosphorous counteracts the
deleterious effect of oxygen on losses.

The silicon-iron laminations used in transformer cores
are in the form of sheets. During rolling of these sheets, however,
along with the deformation of grains, the grains tend to orient
themselves so that a crystallographic plane and a crystallographic
direction respectively align themselves with the rolling plane and
rolling direction. This produces preferred orientation of grains in
the rolled sheets or produces textured material. Hence, one can make
use of this method so as to obtain the right kind of grain
orientation in a suitable magnetic material to produce better
magnetic behaviour. By suitable annealing treatment an entirely
new texture could be produced in deformed metals. Both deformed
as well as annealed materials are useful for laminations in
transformers; but the latter material is more useful for their
increased grain size and lower amount of internal stresses (which
lead to lower losses). Textures also arise from solidification.
In cubic metals, directional solidification can produce columnar
grains which have a [001] direction parallel to the columnar axis[4].

Directional solidification followed by careful hot rolling along the columnar axis retains the [001] direction along the rolling direction[5]. This method, however, does not produce a rolling texture, but produces a fibre texture with [001] direction as the fibre axis.

From the single crystal data on Fe-Si (Fig. 8), it is apparant that the possible orientation of grains for the best magnetic properties will be:

(a)   Cube-on-edge texture (110) [001] in which there will be an easy and a medium-easy directions of magnetization lying on the rolling plane.

(b)   Cube texture (100) [001] in which there will be two easiest directions of magnetization lying on the rolling plane and

(c)   Ideal cold-rolled texture (100) [011] in which there will be two [100] directions at 45° to the rolling direction.

The first two required textures, (110) [001] and (100) [001], can be produced only by a suitable high temperature heat treatment following a suitable cold deformation. The transformation responsible for producing annealing textures is secondary recrystallization of grains, which has its origin in the inhibited normal grain growth of primary recrystallized grains. Weiner[6], May & Turnbull[7], and Walters & Dunn[8] pointed out that the growth of secondary recrystallized grains depends on surface energy character-istics of grains produced in primary recrystallization & the impurities present in the material. Favourably oriented grains, oriented such

that their surface energy is relatively small compared to the other grains, grow at the expense of others. In thin sheets it is easier to produce cube and cube-on-edge textures compared to thick sheets[9]. The presence of certain undissolved impurities is essential for secondary recrystallization to take place, such as N_2[10], MnS[7], TiS[11], CrS[11], VN[12], TiC[13] and VC[14]. The (110) [001] texture was first produced by Goss[15]. A large number of modifications of Goss's process were patented. The process consists of heavy cold rolling of the alloy (the % reduction varies from 75% to 95%[16,17,18] with intermediate annealings and finally annealing at very high temperatures. The method of producing cube texture is so similar to that of the cube-on-edge texture that the conditions under which cube texture is produced are not well understood. Furnace atmosphere has a large effect on the texture produced. O_2[19] and N_2[10] when present in smaller amounts favour the production of cube-on-edge texture, while high vacuum[19] and H_2S[20] tend to produce cube texture.

The third method of producing the required texture is through cold-rolling alone. When bcc metals are cold rolled they invariably produce a rolling texture with [110] direction parallel (with a few degrees deviation) to the rolling direction and (001) plane parallell (with a few degrees to as large as about 45° deviation from the ideal orientation around the {110} direction) with the rolling plane. Along with predominent (100) [011] texture, it is common to find a few minor textures[4], such as {112} <110> and {111} <112> .

B.c.c. metals have been extensively studied for their deformation textures. Especially Mo and Fe-Si alloys have received greater attention than any other bcc metals. Mo[21 to 25] has a pronounced cold rolling texture (001) [011] with a spread around the R.D. and the cross direction. The amount of spread reported by different workers was different. While the amount of spread around the cross direction was reported by all the workers as 5° to 10° only, there is controversy about the spread around the R.D. This spread according to Custers & Reimersa[21] and Semchysen & Timmons[22] is 40° about the R.D. and according to Segmuller and Wasserman[23], only 10° to 20° about the R.D. Texture similar to that of Mo have been obtained for cold rolled W[26], β-brass[27,28], Ti with 18% Nb (bcc)[29], meta stable bcc Zr-Cb alloy[29], Cr rolled at 600°C[30], Ta[23,31] and V[32]. Pugh & Hibbard[31] found (112) [110] minor textures in Ta along with (100) [011] texture. McHargue & Hammond[32] found in V a very similar spread, a similar predominent texture and minor textures as those in Ta.

The general features of the texture of cold-rolled iron are similar to that of Mo. The texture is chiefly one in which <110> directions of grains lie parallel to the rolling direction—with a few degreed deviation—and {001} planes lie in the plane of the rolled sheet, with a deviation from this position chiefly about the rolling direction as the axis. This spread around the rolling direction is nearly 10° to 20°[33] and around the cross direction is about 5° to 7°[33]. Along the cross direction the spread is nearly 45° to 50°. The spread decreases with increasing amounts of reduction[34,35,36]. Certain less predominent textures

were reported by Kurdjumov and Sachs[33] as {112} <110> and {111} <112>. Steels of higher carbon content tend to have less pronounced textures[4].

Si-Fe alloys show similar deformation textures as those of iron. They differ only slightly from unalloyed iron [37 to 39]. The textures are independent of roll diameter, reductions per pass, rolling speed and whether or not the sheet is rolled at 180° to the original rolling direction[37]. Though the cold rolled texture of Fe-Si alloys is independent of the above variables, it is dependent on the actual procedure adopted in cold reduction[38]. Barrett & coworkers[18] reported (100) [011] predominent texture along with {112} <110> and {111} <112> minor textures. This result is similar to that of Kurdjumov & Sachs[33] on pure Fe. May & Turnbull[7] indicated that an intermediate annealing in the process of cold working invariably produces {111} <112> texture in a 2.84% Si-Fe alloy containing Mn (0.11%) and S (0.04%), with negligible amount of carbon (0.006%). Brown[38] indicated that in a single stage cold reduction of a Si-Fe alloy the texture produced is similar to the cold rolled texture of bcc metals i.e. (100) [011] , whereas, a two stage process, i.e. cold reduction through one intermediate annealing, produced complex double texture and in a 3 stage process, i.e. with 2 intermediate annealings, the texture is invariably {111} <112> type. Fiedler[39] indicated that in a 3.25% Si-Fe alloy an intermediate annealing produced a weak component of (110) [001] texture along with {111} <112> texture whereas specimens without intermediate annealing produced {111} <112> texture. Fiedler[39]

also claimed that if a high temperature, of the order of 900° to 1000°C, is employed at the intermediate annealing stage, cube-on-edge texture (110) [001] could be developed in the material.

The textures produced by straight rolling i.e. rolling in the same direction, produces cold rolling textures with varying degrees of spread around the ideal orientations. If a material is rolled in two perpendicular directions, called cross-rolling, the texture obtained is somewhat different from those obtained from the straight rolling method. When the amounts of reductions in two perpendicular directions are roughly equal, the cross rolling texture of bcc metals and alloys is approximately equal to the superposition of two pole figures for straight rolling in two directions[4,21,22]. This result was confirmed by different workers on Mo and Fe. Cross rolling sharpens the cold-deformation texture. Ransley & Rooksby[24] and Smithells[41] observed this in Mo. Ransley & Rooksby concluded that straight rolling of Mo only results in placing one (110) plane perpendicular to the rolling direction. Only after cross rolling the ideal orientation is achieved, a second (110) plane being placed perpendicular to the second rolling direction. Semchyshen & Timmons[22], however, noted that cross rolling brought about a greater spread around the cross direction and a greater concentration of grains with (110) plane parallel to the second rolling direction. Custers & Riemersa[21] as well as Semchyshen & Timmons[22] showed a component with (111) planes parallel to the rolling plane and rotational symmetry about the sheet normal in cross-rolled Mo.

Relatively very small amount of work has been published on the cross-rolled textures of iron and Fe-Si alloys. Hu[42] studied the cross rolled textures of pure iron. The deformation texture was predominently (100) [011] along with minor components of (111) [$\bar{1}10$] or (111) [$11\bar{2}$]. Partial recrystallization makes major texture to retain itself, but minor textures are replaced by new orientations.[42] In a completely recrystallized specimen, a complex and widely scattered texture is developed. These recrystallized textures could be derived from the deformation texture components by rotations around [110] poles. Hu[42] concluded that the difference in the tendency for recrystallization among the different texture components might serve as an important factor in the formation of annealing textures. Wiener & Corcoran[16] confirmed Hu's observation by cold reducing (straight rolling) a Fe-Si alloy and partially recrystallizing it. This procedure produced basically (100) [011] texture with only a small, 0° to 5°, rotation around the cross direction and with a very small {111} <112> texture still remained in the alloy. A complete loss of cold rolled texture resulted if higher temperatures and greater times of annealing were used.

Since the Fe-Si alloys with 3% Si and 3.5% Si, are of importance for the laminations of transformer cores, the present study is confined to the alloys of these compositions. The purpose of the present study was to investigate the effect of cross rolling and subsequent annealing on the textures of these alloy i.e. to see the degree of perfection in texture which can

be achieved by cross rolling, the annealing behaviour of the cross rolled alloys and to study the magnetic properties of the cross rolled and secondary recrystallized Fe-Si alloys.

II EQUIPMENT FABRICATION & CALIBRATION

EQUIPMENT FABRICATION & CALIBRATION

A. Magnetic testing Units

The magnetic measurements required for the Fe-Si alloys are magnetic permeability test, core loss measurements and magnetostriction. Core loss consists of two main components, viz., hysteresis loss and eddy current loss. Permeability and core-loss measuring equipment was designed and fabricated according to the ASTM standard specification: 343 [43] which is equivalent to the IS specification: 649 [44]. Magnetostriction test was not performed.

1. Epstein Test Frame

The dimensions of the test frame are shown in Fig. 9. The frame consists of four solenoids and an air flux compensator mounted on a perspex platform. The details of the frame are given in Table 1. The complete test frame circuit is shown in Fig. 10. The details of circuit components are given in Table 2_A and 2_B. Basically the circuit consists of an ammeter A in the primary circuit to measure current which is directly proportional to the field strength H, a voltmeter V in the secondary circuit to measure the voltage which is directly proportional to the flux density B, and a wattmeter W to measure the power loss. An air-flux compensator is also incorporated in the circuit so that the voltage induced in the secondary of this compensator opposes and balances out the air-flux voltage induced in the secondary winding of the test frame by the primary current. When testing at moderate inductions and low field strengths (where the permeability of the material is high), the air flux compensating inductor is not essential as

TABLE 1.

Components of Epstein test frame

1. Materials of construction.

   Solenoid forms   Bekelite

   Airflux Compensator - Wood

   Platform   - Perspex

2. Solenoid specification.

   Solenoid cross section- 0.875" x 1.375"

   Turns per winding - 175

   Primary winding   - 3 layers with wire size No. 15
                (0.0578")

   Secondary winding - 1 layer with wire size No. 19
                (0.0359")

3. Air flux compensator specification.

   Compersator form - 2" dia x 1" long

   Primary winding   - 4 Layers, 44 turns, with wire size
                No.13(0.072")

   Secondary winding - 425 turns with wire size
                No.19(0.0359")

TABLE 2$_A$

Circuit components & Their Ranges

COMPONENT	RANGE
Ammeter	0-2 amp
Voltmeter	0-75 Volts
Wattmeter	0-75 Watts

TABLE 2$_B$

Switches & their ratings

Switch	Rating
S$_1$, S$_2$, S$_3$	30 Amps
S$_5$, S$_6$	16 amps

the flux density in the air path is negligible[43]. Switches S_1, S_2 S_3 are provided in order to protect the wattmeter, ammeter and the air flux compensator, respectively, when such need arises. The wattmeter and voltmeter are connected to the secondary winding of the test frame through the switches S_5 and S_6 respectively. Though the exciting currents for testing are much less than 1 Ampere, all the switches incorporated in the test frame circuitry have high current ratings (Table 2.3). This is necessary in order to make the contact losses negligible and to avoid appreciable distortion in the sinusoidal wave form of the current drawn. Maintenance of sinusoidal wave form is required if a r.m.s. voltmeter is used to measure the secondary voltage instead of a flux voltmeter. (In the present case r.m.s. voltmeter was used.). The relations between current & field strength and secondary voltage & flux density are given in Appendix I. The power loss measured by the wattmeter also includes power dissipated in the secondary circuit. Hence, to calculate the specific core loss (Core loss per unit mass) for the material, the power loss in the secondary circuit must be subtracted from the total loss.

2. <u>Operation of the Epstein test frame for core loss measurement</u>

The core loss measurement using the standard Epstein test frame was carried out in the following manner: Strips of magnetic material (30.5 cm long and 3 cm wide) of known mass, preferably 2 Kg for better acuracy or smaller amounts preferably not less than 500 gms, were introduced into the four solenoids of the test frame with the strips completely overlapped at the corners so as to constitute a continuous square magnetic circuit. Two successive strips in a solenoid were separated at the ends by two strips from the other two

solenoids perpendicular to it so that no two strips in a given solenoid were in direct contact with each other. The core loss test was performed at flux densities of 10,000 and 15,000 gauss. The secondary voltage needed in order to achieve this induction was calculated using equation 1 of appendix I. With switches S_2, S_4, S_5, S_6 & S_7 closed and S_1 & S_3 open, the primary circuit voltage was adjusted by using a variable voltage auto transformer to the calculated value of secondary voltage. Switch S_3 was opened in order to compensate for the air flux. It was not possible to detect the expected slight changes in the secondary voltage due to opening of switch S_3 with the voltmeter used. Switch S_6 was then opened in order to eliminate the voltmeter load from the circuit and S_3 was once again closed. Now only the resistance of the potential coil of wattmeter acts as the load for the secondary circuit. The wattmeter reading was taken at this stage. Since the resistance of the potential coil, R, is known through the manufacturer's specification (in this case 4800 Ω), the power loss in the secondary circuit, V^2/R, could be calculated. The loss due to the test frame alone was obtained by subtracting the power loss in the secondary circuit from the wattmeter indication. The net loss was divided by the active mass of the strips. The active mass of the strips was calculated on the basis of the active magnetic flux path. For the standard Epstein test frame, the active magnetic flux path was taken as 94 cm according to the specification[43]. Equations for computing the active mass of the specimen and the specific core loss are given in appendix II.

3. Performance tests of the Epstein test frame

The performance test of the fabricated unit has been done in two ways so as to see a) whether the test frame actually matches with the standard specifications and gives satisfactory performance and b) whether the test frame measured losses are reliable. For the first case the specific checks made were to ascertain a) whether the primary to secondary transformation was 1:1 or not, b) whether the typical B-H relationship could be achieved, c) whether saturation could be obtained within the limiting current of the test circuit and d) the nature of variation of permeability as a function of field strength. To check these, the circuit connections were slightly modified as shown in Fig. 11. The tests were conducted with 22 gage (0.031" thick) mild steel strips. The amounts of material put in was varied in a simple ratio of 1:2:3, so that the performance of the frame could be tested for widely varying quantities of material. The test results are plotted in Figs. 12 to 14.

To test the performance of the test frame circuit (Fig. 10) for core loss measurement a set of specimens, for which the losses were known, were utilized. The specimens were supplied by the Rourkela Steel Plant of M/s Hindustan Steel Limited. Test specimens of two thicknesses, 1 mm and 0.5 mm, were utilized for this test. Using the test frame the tests were carried out with 1050 gm of 1 mm thick sheets and 1060 gm of 0.5 mm thick sheets, at flux densities of 10,000 and 15,000 gauss. While performing the magnetic test at these inductions a check was made to see the nature of the wave form of the input voltage and it was found to be sinusoidal (Fig.49). The materials were found to get saturated at around 12,000

TABLE 3.

Magnetic Test data of HSL supplied strips

Set Number	Thickness of strips mm	m, actual mass of specimen, gm	V,* Secondary Voltage, Volts	B, Flux density, Gauss	W, Wattmeter, indication, Watts	R, Resistance of wattmeter potential circuit, Ohms	V^2/R, Watts	Specific core loss Pc, w/Kg**	***Specific core loss as reported by HSL Labs w/Kg	Hysteresis loss Wh, w/kg	(Pc-Wh) eddy current loss We w/kg
I	1.0	1050	17.15	10,000	3.5		0.061	4.28	4.29	1.83	2.45
I	1.0	1050	25.72	15,000	6.5	4,800	0.137	6.63	-	-	-
II	0.5	1060	17.22	10,000	2.0		0.068	2.67	2.63	1.27	1.
II	0.5	1060	25.83	15,000	4.0		0.139	5.44	-	-	-

*   As calculated from equation 1, appendix I .

**   As obtained from our equipment, equation 1, appendix II.

*** H.S.L. labs reported core loss at an induction of 10^4 Gauss only.

indicate an excellent agreement of the values obtained through the present set up and the test result supplied by Hindustan Steel Limited.

The standard test frame circuit was slightly modified to estimate independently the hysteresis loss. To do this the test equipment was hooked up with a Tektronix 503 Oscilloscope as shown in the Fig. 10. The primary circuit was connected to the horizontal input of the oscilloscope through a 1 Ω resistor so that the potential drop, which is numerically equal to the primary current and hence proportional to the field strength, is indicated on the horizontal scale of the oscilloscope screen. Similarly the secondary is connected across a capacitor of 1 μF to the vertical input of the oscilloscope so that the secondary voltage which is proportional to the flux density is indicated on the vertical scale of the oscilloscope. Since the core loss measured on the Epstein test frame was for 10^4 gauss, the same flux density was used for the hysteresis curve tracings (the area of the hysteresis loop increases with increasing levels of flux density, Fig. 15) so as to directly obtain the other losses from the measured ones. While performing this test switches S_1, S_2 and S_3 were closed and S_4, S_6, S_5 and S_7 were opened. Figs. 50 and 51 show typical hysteresis curves for 1 mm and 0.5 mm thick specimens at 10^4 gauss. From the area of the hysteresis loops, hysteresis losses were computed and are shown in the Table 3. The relations between hysteresis loss and the area of the loop are given in Appendix III.

4. Magnetic Test equipment for the study of grain oriented Silicon Steels

A standard test frame for core loss measurement requires

TABLE 4.

Details of Single Solenoid Tester

Length of the Solenoid	–	7.2 cm
Solenoid cross section	–	2.2 x 1.7 cm^2
Turns per winding	–	140
Primary winding	–	8 Layers
Secondary winding	–	1 Layer
Wire size No.	–	28 SWG

large amounts of material and very long specimens. Due to practical
limitations of producing large size specimens of grain oriented
steel in the laboratory and that there was no possibility of
producing large size sheets at the Hindustan Steel Limited plants,
a smaller and simpler test equipment was developed so as to obtain
a relative measure of magnetic properties. · To perform this test a
single solenoid test equipment for showing the hysteresis curves
was designed. The details of the solenoid are given in Table 4.
The circuit diagram is shown in Fig. 11. Preliminary tests using
the Hindustan Steel Limited supplied 0.5 mm hot rolled strips
indicated that the hysteresis loop was slightly distorted and not
well defined since the magnetic flux path in the present case is
an open one. The flux path was closed by using three external steel
strips so that the loop will be better defined. For all the
magnetic tests the same strips were used for completing the flux
path. Keeping the level of induction same, (approximately 8,000
gauss; calculated from equation 1, appendix I), and the mass of the
specimens same (nearly 20 gms) hysteresis loops were recorded for
grain-oriented steels.

III EXPERIMENTAL PROCEDURE

EXPERIMENTAL PROCEDURE

The present studies on grain orientation of Fe-Si were carried out with two important alloy compositions commonly used in power transformer cores, namely, the 3% Si and 3.5% Si-Fe alloys. The experimental work involved were (1) preparation of the required alloys, (2) the analysis of X-ray data which gives the texture of the material and (3) the measurement of electrical and magnetic properties of this material. The procedures adopted for the various steps of experimentation are described in this chapter.

A. Making, Shaping & Heat-treatment of Alloys

1. Melting & Homogenization of Alloys

The starting materials for preparing the pure alloys are electrolytic iron and pure silicon, the compositions of which are given in Table 5. 768 gms of 3% Si and 664 gms of 3.5% Si-Fe alloys were melted in an induction furnace, (Fig. 16) under a protective atmosphere of purified argon. The details of the controlled atmosphere high frequency induction furnace and the gas purification train (Fig. 17) are given by Narula[47]. Before filling the melting chamber with argon gas, the system was evacuated with a rotary pump until a vacuum of 40 μ of Hg was achieved & then the system was flushed with the argon gas so that any contaminants in the system would be carried away. After filling the chamber with argon, the power input to the furnace was slowly increased in steps to 11 Kw. After melting, the alloys were allowed to solidify and cool down to 1150°C in the furnace, annealed for 2 hours for

TABLE 5.

Chemical Analysis

Sl. No.	Material	Composition						
		% Si	% C	% Mn	% S	% P	% O	% N
1.	Pure Iron*	0.01	0.02	-	-	-	-	-
2.	Pure Si*	99.90						
3.	Low Carbon Steel (H.S.L.)**	1.58	0.029	0.21	0.027	0.025		
4.	Pure 3% Si-Fe alloy	2.70	0.10	-	0.01	-	0.005	0.006
5.	Pure 3.5% Si-Fe alloy	3.36	0.06	0.02	0.10	-	0.006	0.007
6.	Comm.purity 3% Si-Fe alloy	2.80	0.07	0.22	0.038			
7.	Comm.purity 3.5% Si-Fe alloy	3.32	0.07	0.2	0.039			

* Supplied by Semi Elements Incorporated, New York.

** Steel supplied by Hindustan Steel Limited, Ranchi.

Commercial purity alloys (Sl.No. 6 & 7 in this table) were

prepared using this steel.

composition homogenization and finally cooled to room temperature
in the furnace. The ingots obtained were approximately 2" dia
and $1\frac{1}{2}$" long. The commercial purity alloys were made from low
carbon steel sheets, supplied by M/s Hindustan Steel Limited
(analysis given in the Table 5). The sheets contained only 1.58%
silicon and hence calculated amounts of pure Si were added in order
to make 3% Si and 3.5% Si-Fe alloys. No addition of pure iron was
made to dilute the alloy with respect to the carbon content for
reasons discussed later. The low carbon steel sheets were cut and
cleaned by 5% HCl to remove the surface oxide and ground to remove
the acid stains before melting. Commercial purity alloys were melted
in a similar way. Nearly 700 gms of 3% Si-Fe and 750 gms of 3.5% Si-Fe
commercial purity alloys were prepared. The ingot surfaces were
machined in order to remove surface defects. The chemical analysis
of all these alloys is also given in the Table 5.

2. Forging of Ingots

The ingots required breaking down of the cast structure as
well as shaping to suitable sizes for the subsequent rolling
operations. The ingots were heated to 1200°C in a Globar muffle
furnace and forged using a power hammer. The forging operation was
carried out in the range of 1150°C to 900°C. The dimensions of the
forged flats are given in Table 6. All the forged flats were cleaned
by grinding. Forged and cleaned pure alloy flats, both 3% Si and
3.5% Si alloys, were cut into approximately $1\frac{1}{2}$" long and 1" wide
pieces. Forged flats of commercial purity alloys were not cut into
smaller pieces.

TABLE 6.

Dimensions of Forged flats and hot rolled sheets

	After gorging After Forging	Dimensions of pieces cut form forged flats	After hot rolling and cutting
Pure Alloys			
3% Si-Fe	14" x 1" x 0.5"	$1\frac{1}{2}$" x 1" x 0.5"	Specimen G
			1" x 1" x 0.109"
			and
			2" x 1" x 0.2"
3.5% Si-Fe	9.2" x $1\frac{1}{8}$" x 0.5"	$1\frac{1}{2}$" x 1" x 0.5"	Specimen A
			2" x 1" x 0.202"
Commercial Purity Alloys			
3% Si-Fe	$5\frac{1}{2}$"x $1\frac{1}{2}$"x 0.4"	Not cut	Specimen F_{comm}
			$1\frac{1}{2}$"x $1\frac{1}{2}$"x 0.2"
3.5% Si-Fe	5" x $1\frac{1}{2}$"x 0.4"	Not cut	Specimen F_{comm}
			$1\frac{1}{2}$"x $1\frac{1}{2}$"x 0.2"

3. Hot rolling of forged specimens

Since hot rolling required an operating temperature of 900°C to 1200°C, the specimen had to be heated to these high temperatures using the 'Globar' muffle furnace. This furnace had space limitation in that the final length of the rolled material had always to be within 6". This was the reason for cutting the pure alloy flats into smaller pieces before hot rolling. Commercial purity alloy flats were hot rolled along the breadth of the flats so that the material does not exceed 6" in length during hot rolling. During heating of pure alloy pieces to the required hot rolling temperatures surface oxidation was minimised by heating up to 950°C in a controlled atmosphere furnace[47], followed by heating in the Globar furnace which was maintained at 1200°C. The hot rolled sheets were cut into smaller pieces of the dimensions given in the Table 6. The edges of these pieces were ground so as to remove the microcracks that may be present at the edges. This is needed because these minute cracks may propogate while cross rolling operation is carried out.

4. Cross rolling

Cross rolling of alloys was done by rolling the material in two perpendicular directions. The original direction of rolling (during hot rolling) is called here the rolling direction and the perpendicular direction as the cross direction. Since texture developed during cold rolling changes characteristics if rolling directions vary, it is essential to keep the rolling directions same, i.e. to prevent accidental rolling at an angle to the actual rolling direction. To achieve perfect roll feeding an adjustable guide, Fig. 18, was used. The details of the guide are given by Narula[47]. The 3% Si-Fe

alloy could be cross rolled safely at room temperature. On the other hand the 3.5% Si-Fe alloys were found to be prone to cracking on cross rolling. Hence all cross rolling was done between $200^\circ C$ to $350^\circ C$. It was observed that 3% Si-Fe commercial purity alloy was more brittle compared to pure alloy of the same composition. Hence commercial purity 3% Si-Fe alloy was also cross rolled in the same range of temperatures. The reduction in each pass was maintained at 0.005" for all specimens of all compositions.

5. Specimen thinning

Thinning of specimen was done after cross rolling. The final thickness of cross rolled products varied between 0.014" to 0.025". Specimens were thinned to about 0.003" before taking X-ray data. The Goniometer used for X-ray data was of transmission type and hence to achieve a reasonably high intensity of the diffracted beam specimen had to be thinned. Thinning of 3% Si-Fe alternate cross rolled specimen was done by careful mechanical polishing from 0.025" to 0.006" and finally 5% Nital was used to etch the material till a thickness of 0.003" was obtained. Thinning by mechanical polishing is time consuming, laborious and requires care in maintaining the evenness of the specimen surface. Hence electrolytic and chemical thinning techniques were tried (Table 7_A & 7_B), and finally a solution containing 30% HCl, 30% HNO_3, 30% water and 10% CH_3COOH was found to be most suitable for initial thinning of the specimen. All the other specimens were thinned by using this solution to about 0.005" to 0.006" and finally 5% Nital was employed to remove small amounts of surface layers. The specimen surfaces were cleaned with acetone and studied for the X-ray data.

TABLE 7 A

Electrolytic thinning solution and its Characteristics

No.	Composition of Electrolyte	Electro thinning conditions		Performance and characteristics
		Current density c.d. amp/cm^2	Voltage Volts	
A	Citric acid 10gm Na Cl 100gm HCl Few ml H_2O 1000 cc	8-10	10-13	Fast reaction, very rapid reaction at the specimen edges. Minute pits formed

TABLE 7 B

Chemical thinning solutions used and their characteristics

No.	Solution	Performance and characteristics
B	HNO_3 5% Alcohol 95%	Very slow reaction, composition changes rapidly due to evoporation of alcohol, suitable for removal of small amount of material.
C	HNO_3 - 30% HCl - 30% CH_3COOH - 10% H_2O - 30%	Very fast reaction, uniform thinning of specimen all over; no preferencial reaction at the edges; No pit formation
D	Saturated solution of oxalic acid in H_2O_2	Fast; but relatively slow reaction compared to solution C; no preferential attack at edges; surface becomes uneven after thinning

6. Annealing of cross rolled & thinned specimen

After collecting the X-ray data on as-cross rolled &
thinned specimens, the specimens were annealed in a vacuum furnace,
Fig. 19. The furnace has been described in detail by Band[46]. The
required vacuum of about 50 torr was obtained by a rotary pump. The
specimens were introduced into the hot zone (without breaking the
vacuum) with the help of a strong permanent magnet. The pure as well
as commercial purity 3% Si-Fe alloys and 3.5% Si commercial purity
alloys were annealed at 400°C for $2\frac{1}{2}$ hours; the pure 3.5% Si-Fe
alloys were annealed at 550°C for $\frac{1}{2}$ hour. The annealed specimens were
studied for the X-ray data.

B. X-ray studies for texture determination

1. Evaluation of Bragg angle $\phi(110)$ and μt of each specimen

The texture determination requires keeping the counter at the
correct Bragg angle position for a given (hkl) reflection. Hence one
requires the correct value of $\theta(hkl)$. Since (110) reflection was chosen
for texture work for both 3% Si and 3.5% Si alloys $\theta(hkl)$ was determined
by powder diffraction technique. Mo radiation was used for this purpose.
The $\theta_{(110)}$ of these two alloys were calculated by determining the
lattice parameter corresponding to each of these alloys.

It is customary to determine the product of the absorption
coefficient and the thickness of the specimen, i.e. μt, by experiment
rather than by calculation. The value of μt is to be known in order
to evaluate the correction factors for the measured intensity of
diffracted beams of different positions of α-rotation. The evaluation
of μt is done by first obtaining a monochromatic beam from any

specimen (in our case parma quartz) and measuring the intensity of the diffracted beam, Io. By inserting the specimen in the path of diffracted beam, to act as an absorber, the intensity of the transmitted diffracted beam, I, is remeasured. The two intensities are related by the equation:

$$I = Io \ e^{-\mu t}$$
$$or \ \mu t = In \ (^{I}/Io)$$

2. Texture determination

For a given Fe-Si specimen the counter was set at the correct $2\theta(110)$ and the specimen (mounted on the goniometer (Fig. 20) whose details of design, construction and calibration are given by Band[46]) was set bisecting the angle between the incident beam So and diffracted beam S (Fig. 21). For the present work, the diffractometer conditions found most suitable were the following:

Slit at source - 1° MR sollar slit.

Slit at counter - 0.2° and MR sollar slit,

Counter - Scintillation counter.

Voltage - 35 KVP

Milliampres - 15 mA

Preset time - 100 secs.

The counter used for obtaining data on commercial purity alloys was a proportional counter whose counting efficiency was much less than that of the scintillation counter which was used for the pure Fe-Si alloys. Specimens were oscillated with the help of a 1 r.p.m. reversible synchronous motor. When the texture is strong with cross rolled specimen the preliminary tests indicated only very slight change in the intensity measured whether the specimen was oscillated or not.

Since the electrical device for specimen oscillation failed at the later part of the work the commercial purity alloys data was taken without specimen oscillation. For obtaining data of $\frac{1}{4}$th of the pole figure specimen was rotated through θ and ϕ from 0° to 50° and 0° to 90°, respectively. The measured intensities were corrected using the correction charts shown in Figs. 24 & 25 The corrected values were plotted on the polar net and contours joining equal intensity points were joined. The method of plotting is shown in Fig. 22. With the help of the standard stereogram (Fig. 23) the texture was determined.

C. Magnetic measurements

Hysteresis loss measurements were made using 3% as well as 3.5% Si-Fe commercial purity alloys - cross rolled, straight rolled[46] recrystallized[46] and cross rolled & partially recrystallized. Since the standard test equipment could not be used for magnetic tests the modified test set up,(Fig. 11), had to be used for plotting the B-H curves for comparison purposes. The test specimens of equal masses were introduced into a single solenoid and the magnetic flux path was closed by using three steel strips. The same strips, for completing the flux path, were used for all the tests. The areas of the hysteresis loops were measured using a planimeter.

D. Resistivity Measurements

Resistivity of Fe-Si alloys is an important parameter, since eddy current losses depend on the resistivity of the alloys (with increasing resistivity, eddy current losses decrease). Therefore, resistivity measurements on the straight rolled 3.5% Si-Fe commercial

of the rolled sheet. Specimens were made by cutting the straight rolled 3.5% Si-Fe commercial purity alloy[46] along the rolling direction and at 45° to the rolling direction. According to the ASTM standards, the length of the specimens should be at least 10 times that of the width. In the present case the ratio of the length to width was about 20. Resistance of these specimens was measured using a Kelvin bridge (Make: Leeds & Northrup; Type: 4300) at a temperature of 21.2°C. Resistivity was calculated using the values of the resistance, length of the specimen and average value of the area of cross section of the specimens. Width and thickness of the specimens were measured at 8 to 12 points on the length of specimens (approximately 4.5 cm) so that an accurate assessment of the area of cross section could be made.

IV RESULTS AND DISCUSSION

Four iron-silicon alloys, namely, pure and commercial purity
3% Si and 3.5% Si-Fe alloys, were studied to determine the effects of
cross rolling (and subsequent annealing of cross rolled product) on
the deformation texture and to determine the magnetic properties of
these alloys.   The details of the cross rolling, heat treatment and
texture data of these alloys are given in Tables 8_A, 8_B, 9_A and 9_B
and shown in Figs. 28 to 44.   The magnetic properties of sheets
(hysteresis curves) are shown in Figs. 52 to 60 and the hysteresis
loop areas are shown in Table 12.

The samples of pure alloy were prepared with low carbon,
low silicon steel supplied by Rourkella Steel Plant of Hindustan
Steel Ltd., Ranchi. The steel contained a higher carbon content
(0.029% C) than what is normally desired (< 0.01% C) in grain-
oriented alloys. The alloys prepared on analysis, however, indicated
reasonable ammount of carbon pick up which is due to the graphite
susceptor used in the induction furnace and the long heat treatment
given in the same furnace. Increased carbon has two fold effect, viz.,
a) it increases the hysteresis losses (Fig. 7) and b) it affects the
γ - loop of Fe-Si binary system (Figs. 26 & 27). Small changes
in carbon content can change large extension of the undesirable
γ and $(\alpha + \gamma)$ region. In the present case, however, the externsion
of $(\alpha + \gamma)$ region is not important because only cold rolling and
low temperature annealing are involved. From Fig. 7, it can be noted
that the variation in the hysteresis losses with increasing carbon
content in the range of 0.01% C to 0.07% C, is small compared to that
in the range of 0 to 0.01% C. Thus the material under study, even

TABLE 8 A

Cross roling schedule of pure 3% and 3.5% Si-Fe alloys

Specimen		Hot rolling	Cross rolling		
Comp-osit-ion	Desig-nation	thickness	Schedule	Final Thickness	% red
		0.109 "	Alternate Cross rolling	0.025"	77
3 % S$_i$	G	0.2 "	SR:CR= 3:1	0.017"	92
		0.2 "	SR:CR 3:1 upto 0.025" followed by SR	0.017"	92
			Alternate CR	0.017"	91
		0.202" Cold rolled to 0.104" by			
3,5%	A	SR	SR:CR 3:1 from 0.104" to 0.025" followed by SR to final thickness	0.014"	92

SR- straight rolling

CR- cross rolling

TABLE 8$_B$

Cross rolling schedule of commercial purity

3% Si and 3.5% Si-Fe alloys

Specimen			Cross Rolling		
Composition	Designation	Final hot rolled thickness	Schedule	Final thickness	% Red.
3% Si	E$_{Comm}$	0.2"	Alternate cross Rolling	0.014"	93
			3:1=SR:CR	0.014"	93
3.5% Si	F$_{Comm}$	0.2"	Alternate Cross Rolling	0.014"	93
			3:1=SR:CR	0.014"	93

Note: a) While cold rolling specimen temperature was 200°C to 350°C.

b) Reduction per pass = 0.005" for all specimens while cold rolling.

though had a larger amount of % C, is not expected to have too high an increase in the losses compared to the starting material (H.S.L. supplied steel). For alloys of commercial importance it is however desirable to keep carbon content as low as possible, preferably below 0.01%. The Mn, S and P contents of the alloy are also slightly higher than what is normally preferred in grain-oriented alloys. Slightly higher Mn and P are not harmful because Mn has little effect on losses, while P decreases the losses considerably.

The ideal cold rolled texture (100) [011] will show three intensity maxima, at a) $\phi = 0°$, $\alpha = 0°$, i.e. coincident with the cross direction (C.D.), b) $\phi = 90°$, $\alpha = 0°$, i.e. coincident with the rolling direction (R.D.) and c) $\phi = 45°$, $\alpha = -45°$ which has been called the central peak. According to the general convention, the textures were interpreted in terms of the ideal texture even when there was considerable spread around or deviation from the ideal texture. Spread of intensity indicates deviations of the required crystallographic planes and directions from the ideal ones. Since there is no absolute basis for comparing the spread of intensity in different pole figures, it has been expressed in terms of angular distance (from the ideal positions) at which the intensity falls to one-third of that at the ideal positions. The spread observed in different pole figures is given in Table 10.

As was mentioned earlier (Chapter I), very small amount of work has been published regarding the cross rolling textures of bcc metals, in particular Si-Fe alloys. Hu's[42] work on pure iron indicates a sharpening of the (100) [011] texture due to alternate cross rolling. In the present investigation the 3% Si-Fe pure alloy

TABLE 9 A

Heat treatment and Texture data for cross rolled pure
Si-Fe Alloys.

| Specimen Designation | Annealing | | Pole figure | Texture in (110) pole figure |
	Temp. in °C	Time in hrs		
	–	–	Fig. 28	Very strong (100) [011] texture but with a minor texture peak at 38° from C.D. Peak intensities are more or less of equal intensity. Central peak displaced by about 5°.
	–	–	Fig. 29	Very strong (100) [011] texture but with a very weak minor texture at about 40° from C.D. Pole density more at R.D. than at C.D. and centre
G	400	2½	Fig. 30	Very strong (100) [011] texture but showing considerable spread along the cross direction. Pole density more at R.D. than at C.D. and centre. Weak minor texture still present. Centre peak displaced by about 4°.
	–	–	Fig. 31	Very strong (100) [011] texture but pole density more at R.D. than at C.D. and centre. No minor texture observed. Large spread along C.D.
	400	2½	Fig. 32	Very strong (100) [011] texture but slightly weaker than cold rolled state. No minor texture observed. Pole density more at R.D. than at C.D. and centre. Spread retained.
	–	–	Fig. 33	Very strong (100) [011] texture; Almost equal intensity peaks; No minor texture found. Spread is very small.
	550	2½	Fig. 34	Weak (100)[011] texture with pole density at C.D. and centre more than at R.D. Minor texture peaks found.
A	–	–	Fig. 35	Very strong (100){011] texture, pole density at R.D. very high compared to C.D. and centre. A strong peak at 30° along C.D. line. Spread along C.D.
	550	2½	Fig. 36	Random texture. Peaks displaced. All peaks are of very low intensity

TABLE 9$_B$

Texture of cross rolled and subsequently heat treated

Commercial purity Si-Fe alloys

Specimen Designation	Annealing Temp. in °C	Time in hrs	Pole figure	Texture in (110) pole figure
	-	-	Fig. 37	Very strong (100) [011] texture. The intensies at the ideal positions are of equal level. A minor texture observed. Spread reasonable.
	400	2½	Fig. 38	Very strong (100)[011] texture; intensities of the peaks increased compared to cold rolled state. No minor texture observed.
E$_{Comm}$	-	-	Fig. 39	Very strong (100)[011] texture, but pole density more at R.D. than at C.D. and centre.
	400	2½	Fig. 40	Very strong (100) {011} texture; peaks at R.D. and C.D. displaced by 2°. Intensities of peaks increased compared to cold rolled state. A weak minor texture peak at about 33° from C.D. appears.
	-	-	Fig. 41	Very strong (100)[011] texture. Pole density ⋯ l.ost equal at the ideal position. ~~A weak minor peak observed at 40° from C.D.~~
	400	2½	Fig. 42	Very strong (100)[011] texture. retained peak intensities at R.D. increased compared to cold rolled state and at C.D. and centre decreased. Minor peak still remained without displacements and changes in intensity.
F$_{Comm}$	-	-	Fig. 43	Very strong (100)[011] texture. Pole density at R.D. is very high compared to C.D. and centre. Spread is more at C.D.
	400	2½	Fig. 44	Very strong (100)[011] texture retained. The intensity difference between R.D. and C.D. positions decreases compared to cold rolled state. Spread at C.D. decreased while it increased at R.D. A weak minor peak at 31° from C.D. observed.

TABLE 10.

Amounts of Spread* of intensities for different specimens

S.No.	Specimen and Treatment	Pole Figure Number	SPREAD AROUND C.D.	AROUND R.D.	ALONG C.D.	ALONG R.D
1.	3% Si-Fe, G, Alternate C.R.	28	10°	5°	7°	4°
2.	G, SR:CR=3:1	29	8°	8°	20°	6°
3.	G, SR:CR=3:1 annealed	30	15°	8°	15°	5°
4.	G, SR:CR=3:1, followed by SR	31	10°	6°	40°	7°
5.	G, SR:CR=3:1, followed by SR, annealed	32	10°	8°	24°	6°
6.	3.5% pure Si-Fe, A_b, SR***	-	25°	35°	13°	15°
7.	3.5% Si-Fe, A, alternate CR	33	8°	4°	6°	3°
8.	A, alternate CR, annealed	34	22°	8°	Very	high
9.	A, SR:CR=3:1, followed by SR	35	10°	6°	40°	4°
10.	A, SR:CR=3:1, followed by SR, annealed	36	Random	Texture		
11.	3% Si-Fe, $E_{comm,}$ alternate CR	37	8°	10°	8°	6°
12.	$E_{comm,}$ alternate CR, annealed	38	8°	8°	7°	7°
13.	$E_{comm,}$ SR:CR=3:1	39	15°	8°	20°	4°
14.	$E_{comm,}$ SR:CR=3.1 annealed	40	15°	8°	20°	6°
15.	3% Si-Fe, $C_{comm,}$ SR**	-	7°	10°	6°	11°
16.	3.5% Si-Fe, $A_{comm,}$ SR***	-	13°	15°	4°	5°
17.	3.5% Si-Fe, $F_{comm,}$ alternate CR	41	10°	9°	10°	10°
18.	$F_{comm,}$ alternate CR, annealed	42	10°	12°	10°	7°
19.	$F_{comm,}$ SR:CR=3:1	43	20°	10°	20°	8°
20.	$F_{comm,}$ SR:CR=3:1, annealed	44	10°	8°	25°	16°

* Spread is taken as the angular distance at which the respective peak intensities fall to 1/3rd of their value at C.D. and R.D.

** Data from Narula[47]   *** Date from Band[46]

(specimen G) on alternate cross rolling showed a very strong cold rolled texture, (100) [011] . The central peak, however, was found shifted by about 5° and a minor texture peak appeared at about 38° from the cross direction (Fig. 28, Table 9$_A$). The spread of the (110) poles (Table 10) in this case was found to be reasonable (5° to 10°). For the 3% Si-Fe alloy the change in texture produced by cross rolling compared to straight rolling could not be studied because alloy with the same amount of reduction by straight rolling was not available.

The 3.5% pure Si-Fe alloy (Specimen A), before alternate cross rolling, was given a 50% reduction by straight rolling. After cross rolling (total reduction 91%) the specimen exhibited a very strong texture with very high intensity peaks of almost equal intensities at the three ideal positions (Fig. 33, Table 9$_A$). The spread was very small and no minor texture was observed. A straight rolled alloy of the same composition and the same amount of reduction[46] showed a considerable spread of intensities (Table 10) indicating that for 3.5% Si-Fe alloys cross rolling sharpens the (100) [011] texture. As far as cross rolling is concerned it is not known whether 3% Si and 3.5% Si-F$_e$ alloys will behave in a similar manner. Hence, if the texture produced due to cross rolling is independent of the alloy composition, then in the 3% Si-Fe alloys straight rolling followed by alternate cross rolling is expected to produce sharper texture.

Like the pure Fe-Si alloys, both the commercial purity alloys (Specimens E$_{comm}$ & F$_{comm}$) on cross rolling showed very strong texture (100) [011] with small spread of intensities (Figs. 37 and 41 and Table 10) around the ideal (110) pole locations. Inspite of the

heavy reduction (93%) the commercial purity 3% Si-Fe alloy showed the presence of a low intensity peak at 40° from the cross direction. This peak, which is due to some minor texture, was found at the same position as in the specimen G (Fig. 28) but was comparatively much weaker. The 3.5% commercial purity Si-Fe alloy did not show clearly any minor peak as was observed in the case of 3.5% pure Si-Fe alloy. Comparison of the texture produced in straight rolled [46,47] and cross rolled commercial purity alloys indicate that the cross rolled textures are as sharp as the texture of straight rolled 3% Si-Fe alloy[47] (Specimen C_{comm}) and more pronounced than the texture of straight rolled 3.5% Si-Fe alloy (specimen A_{comm}). These results indicate that the cross rolled alloys show, in general, a sharper texture compared to the straight rolled alloys and the relative improvement of texture in 3.5% Si alloy (comparing the sharpness of texture between straight and cross rolled material) is better than in the case of 3% Si alloy.

In the literature there is no indication of the effects produced by different degrees of cross rolling, possibly because this method of producing grain-oriented steel is not very popular commercially. In order to find the effect of different degrees of cross rolling on the texture of Fe-Si alloys, an attempt was made to study the effect of 3:1 cross rolling (SR:CR = 3:1) in which for every three passes in the original rolling direction (the hot rolling direction) one pass was given in the perpendicular or the cross direction. All alloys were subjected to the 3:1 cross rolling. The common characteristics of textures produced by the 3:1 cross rolling were 1) the (100) [011] texture produced was very strong in all cases, but the pole density at the rolling direction became very high

(about 2 to 3 times) compared to the cross direction and the centre,
2) while the spread along the cross direction became quite large
(about 20° to 45°), the spread at the rolling direction was quite small
(4° to 10°). The 3% pure Si-Fe alloy on 3:1 cross rolling showed a
weak minor texture at about 40° from the cross direction (Fig. 29) but
the commercial purity 3% Si as well as 3.5% Si alloys, for the same
rolling treatment, were free from minor textures (Figs. 39 & 43).
The 3:1 cross rolled texture of 3.5% Si-Fe pure alloy (specimen A)
could not be studied because the specimen developed pin holes during
thinning. Since the texture produced by 3:1 cross rolling produced
symmetry in the pole densities at the ideal locations of the
(110) poles, a 3:1 treatment followed by straight rolling was tried
to see whether or not the intensities at the cross direction and at
the centre can be increased. This treatment on specimen A showed a
very large difference in the pole densities at the cross and the rolling
directions; the ratio of intensities being as high as 6. Moreover,
it produced a reasonably strong minor texture peak. The 3% Si-Fe alloy
(specimen G), rolled in the same manner, showed an increased spread of
intensities along the cross direction and at the centre compared to
the same alloy which was subjected to only 3:1 cross rolling. In this
case also there was an increase in the ratio of intensities measured at
the rolling direction and the cross direction.

The present cross rolling data together with the straight
rolling data of Narula[47] and Band[46] thus indicate that either
straight rolling or alternate cross rolling produces strong cold
rolled texture, (100) [011] . The increased intensity at the
rolling direction and decreased intensity at the cross direction and

the centre due to a higher ratio of straight to cross rolling indicate that the rolling texture tends to become more like a fibre texture and the maximum asymmetry due to partial randomness (if not complete randomness) around the rolling direction is expected at some specific straight to cross rolling ratio. This critical ratio of straight to cross rolling, however, was not determined.

Cross rolled material in the as-cold rolled state has lattice imperfections and residual stresses. These stresses must be relieved by annealing in order to make the material more stable. The time and temperature of annealing must be carefully chosen in order to avoid change or loss of texture which was produced by cold rolling. In order to find the most suitable time and temperature for annealing the 3:1 cross rolled specimens were annealed at 400°C and 550°C for various lengths of time and microstructures were examined. At 400°C a $2\frac{1}{2}$ hour annealing and at 550°C a $\frac{1}{2}$ hr anneal produced about 60% recrystallization (Fig. 45 to 48). Since the purpose of anneal was to remove the stresses produced due to cold work this amount of recrystallization was considered suitable for the present study and all alloys were annealed at either of these temperatures. In all alloys, except for the 3% Si-Fe pure alloy, the cross rolling followed by 400°C annealing did not produce significant change in the ratio of intensities at the rolling and the cross directions ($I_{R.D}/I_{C.D}$) and the texture produced by cross rolling was retained (Figs. 30, 32, 38, 40, 42 and 44) and Tables 9 and 10). The 3% Si-Fe pure alloy while retained the strong cross rolled texture, showed a considerable increase in the ratio $I_{R.D}/I_{C.D}$. The minor peaks

observed in the 3:1 cross rolled specimen G (Fig. 30) and alternate cross rolled specimen F_{comm} (Fig. 42) were retained after annealing and in the case of 3:1 cross rolled commercial purity alloys a new peak due to secondary texture was observed at 30° from the cross direction. On the other hand the annealing at 3:1 cross rolled and alternate cross rolled 3.5% Si-Fe pure alloy at 550°C produced a complete random texture (Fig. 34 & 36) with a few secondary peaks due to textures other than the cold rolled texture.

Annealing behaviour of cross rolled pure Fe and straight rolled Si-Fe alloys has been studied by Hu[42] and Corcoron.[16] Hu[42] observed that the cross rolled pure Fe on annealing at 550°C produced sharpening of the cold rolled texture but a completely random texture is produced at 675°C due to complete recrystallization. The progressive loss in texture was related to the progress of recrystallization. Corcoron[16] also arrived at the same conclusion. The microstructures of alloys (this investigation) annealed at 400°C and 550°C, however, show that there is no significant difference between the amount of recrystallization produced in the two cases. Hence, the loss of texture in one and retention of texture in another does not seem to depend on the amount of recrystallization produced. The annealing behaviour of 80% cold rolled (100)[011] oriented single crystals of 3.12% Si-Fe alloy (rolled along the [110] direction) showed[48]:

1)   Very strong (100)[011] deformation texture.

2)   Practically no effect on properties due to annealing below 400°C.

3)   At and above 400°C (upto 1200°C) the material

softened but did not recrystallize.

4)   Sub-grains formed and grew in size as temperature was raised above 400°C.

From these observations it will be clear that since there is no recrystallization the texture of annealed material should remain (100) 011 and from this point of view the retention of cold rolled texture at 400°C will be justified. The microstructural change produced has tobe interpreted as the formation of subgrains. However, from this point of view there should not be any change in texture due to annealing at 550°C. Since there is a complete loss of texture at 550°C it would mean that the results obtained on the single crystals are not applicable for polycrystalline material. The work of Band[46] and Narula[47] on straight rolled Fe-Si alloys also indicated that the effect of annealing in the temperature range at 700° – 950°C is to produce randomisation of texture, the effect being more for the 3% Si alloy than for the 3.5% Si alloy. The microstructural change at 400°C and 550°C indicate that the material is going through partial recrystallization rather than through subgrain formation. At 400°C the crystallized grains seem to be of the same orientation as the matrix, i.e. (100) [011] whereas the recrystallized grains produced at 550°C appears to be randomly oriented and thereby causing a complete loss of texture.

Resistivity of electrical sheets, being an important parameter in controlling the eddy current losses, as high as possible. The resistivity values for Si-Fe sheets are available in the ASTM standards specification[43]. The resistivity of the two alloys prepared were measured. These measurements indicate that the resistivity values

TABLE 11

Resistivity Measurements

Composition	Treatment	Resistivity microohm – cm		ASTM* Data
		Cut at 45° to R.D.	Cut along R.D.	
3.5% Si–Fe commercial purity alloy	Straight rolled	56.12	54.60	53

* Reading from . resistivity Vs composition curve.

obtained in the $[\bar{1}00]$ and $[011]$ directions are nearly equal and slightly higher than the values given in the ASTM specification. This increase in resistivity may be attributed to the higher carbon content and the presence of other impurities.

The single solenoid magnetic test was used in order to assess the relative hysteresis losses of commercial purity as-rolled and heat treated alloys. Since the test equipment and the test procedure are not standard ones, in order to make the results meaningful and comparable with each other, the variable parameters in testing, the mass and the length of the specimens, test induction, oscilloscope settings, were all kept the same. The straight rolled [40] and cross rolled sheets were cut at 45° to the rolling direction so that the specimens obtained can be tested with their direction of easy magnetisation, $[\bar{1}00]$, aligned with the field. The straight rolled sheets were also cut along the rolling direction, in order to bring the medium easy direction of magnetization $[011]$ along the field, so that the hysteresis loss of these sheets could be compared with that of the 45° cut sheets.

One set of secondary recrystallized specimen in the cube-on-edge texture (110) $[00\bar{1}]$ [46] was cut along the rolling direction so that the $[00\bar{1}]$ was parallel to the solenoid axis. The cross rolled specimens, annealed at 400°C for $2\frac{1}{2}$ hours were also tested in order to see the effect of annealing on the losses. The results obtained indicate that 1) inspite of the fact that the commercial purity alloys contained a large amount of carbon (0.07%) the hysteresis loops for the 45° cut alloys (both 3% Si and 3.5% Si) were found to be very similar to that of the H.S.L. supplied 0.5mm thick sheet specimens. 2) the

TABLE 12.

Magnetic Test Data on oriented Commercial Purity Si-Fe Alloys

S.No.	Composition	Designation	Treatment	Area of hysteresis loop, in Sq. in x 10^{-2}	Corresponding Figure
1.	–	H.S.L.Supplied 0.5 mm thick specimens	Hot rolled	105	–
2.	3.5% Si-Fe	*A.comm	Cold(straight) rolled, cut along R.D.**	107	52
3.	"	"	Cold(straight) rolled, cut at 45° to R.D.	104	53
4.	"	"	Straight rolled, cut along R.D., Annealed at 1150°C for 4 hrs.	98	54
5.	3.5% Si-Fe	Fcomm	Alternate cross rolled, cut at 45° to R.D.	102	55
6.	"	"	Same as above specimen, but annealed at 400°C for $2\frac{1}{2}$ hrs.	82	56
7.	3% Si-Fe	Ecomm	Alternate CR, cut at 45° to R.D.	105	57
8.	"	"	Same as above specimen, but annealed at 400°C for $2\frac{1}{2}$ hrs.	92	58
9.	3% Si-Fe	Ecomm	SR:CR = 3:1 cut at 45° to R.D.	99	59
10.	"	"	Same as above specimen, but annealed at 400°C for $2\frac{1}{2}$ hrs.	83	60

* Specimens received through the work of Band[46].

secondary recrystallized specimen show slightly lower values of the losses than the as-rolled, (cut at 45°) sheets; this is expected because the recrystallized specimens have lower residual stresses,

3) On annealing the cross rolled (45° cut) specimens show an appreciable decrease in the hysteresis loop area due to the elimination of residual stresses and lattice imperfections.
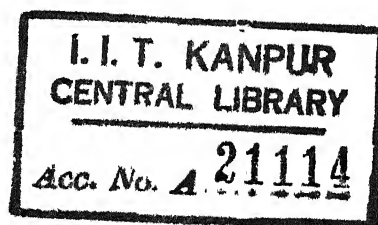
CONCLUSIONS

From the present investigation of pure and commercial purity 3% Si and 3.5% Si-Fe alloys the following conclusions can be drawn:

1) Cross rolling sharpens the cold rolled texture, i.e. $(100)[01\bar{1}]$ texture of Si-Fe alloys.

2) 3:1 cross rolling brings in unequal pole densities at the rolling and the cross directions.

3) Annealing of cross rolled product at 400°C for $2\frac{1}{2}$ hours basically retains the cross rolling texture, i.e. $(100) [01\bar{1}]$ texture.

4) Annealing of cross rolled product at 550°C for $\frac{1}{2}$ hour destroys the as-cross rolled texture.

5) Annealing at 400°C decreases the hysteresis losses considerably.

REFERENCES

References

1. S. Kaya & Hunda, Sc. Repts., Tohoku Imp. Univ. 15, 721, 1926.

2. H.J. Williams, Phy. Rev, 52, 747, 1937.

3. R.M. Bozorth, Ferromagnetism, Van Nostrand Co, Inc., 1951.

4. C. Barett & T.B. Masalski, Structure of Metals, McGraw Hill, Inc., 1968.

5. J.L. Walters & W.R. Hibberd, See E. Adams, J. Appl. Phys, 35, 856, 1964.

6. G. Wiener, J. Appl. Phys, 35, 856, 1964.

7. J.E. May & D. Turnbull, Trans. AIME, 212, 769, 1958.

8. J.L. Walters & C.G. Dunn, Acta. Met, 8, 497, 1960.

9. Magnetism & Metallurgy, ed. by E. Berkowitz & E. Kneller, Vol. 3, Academic Press, 1969.

10. W. Morill, Metal Progress, 54, 675, 1948.

11. J.E. May & D. Turnbull, J. Appl. Phys, 30, 2105, 1959.

12. H.C. Fiedler, Trans. AIMME, 221, 1201, 1961.

13. H.C. Fiedler & R.H. Pry, U.S. Pat. 2, 939,810, 1960.

14. E.V. Walker & J. Howard, Powder Met, 4, 32, 1959.

15. N.P. Goss, Trans. ASM, 23, 511, 1935.

16. G. Wiener & L. Corcoron, J. Metals, 8, 901, 1956.

17. B.F. Deaker & D. Harker, J. Appl. Phy, 22, 900, 1951.

18. C.S. Barett, Ansel & R.F. Mehl, Trans. AIME, 125, 516, 1937.

19. P.B.Mee, Trans. Met. Soc. AIME, 242, 2155, 1968.

20. Kramer, Sec E. Adams, J. Appl. Phys, 35, 1964, 856.

21. J.F. Custers & J.C. Reimersa, Physica, 12, 195, 1946.

22. M. Semchysen & G.Timmons, J. Metals, 4, 279, 1952.

23. A. Segmuller & G. Wasserman, Trans. AIME, 194, 745, 1952.

24. C.E. Ransley & P.Rookshy, J. Inst. Metals, 62, 205, 1938.

25. N. Ujiije & R. Maddin, J. Metals, 8, 1298, 1956.

26. J.W. Pugh, Trans. AIME, 212, 537, 1958.

27. W. Iweronowa & G. Schdanow, Tech. Phys. USSR, 1, 64, 1934.

28. H. Asada & E. Tanaka, Rep. Inst. Sci. Technol., Tokyo, 6, 13, 1952.

29. J.H. Keeler, Trans. AIME, 206, 122, 1956.

30. W.H. Smith, J. Metals, 7, 1064, 1955.

31. J.W. Pugh & W.Hibbard, Trans. ASM, 48, 526, 1956.

32. C.J. McHargue & J.P. Hammond, Trans. AIME, 194, 745, 1952.

33. G. Kurdzumow & G. Sachs, Z. Physik, 62, 592, 1930.

34. C.B. Post, Trans. ASM, 24, 679, 1936.

35. D.L. McLachlan & W.P. Davey, Trans. ASM, 25, 1084, 1937.

36. M. Gensamer & R.F. Mehl, Trans. AIME, 120, 277, 1936.

37. W.A. Sisson, Metals Alloys, 4, 193, 1933.

38. J.R. Brown, J. Appl. Phys, 29, 359, 1958.

39. H.C. Fiedler, J. Appl. Phy, 29, 361, 1958.

40. F. Haessner & H. Weik, Arch. Eisenhuttenw, 27, 153, 1956.

41. C.J. Smithells, J. Inst. Metals, 60, 172, 1937

42. Hsun Hu, J. Metals, 9, 1164, 1957.

43. A.S.T.M. Standards, part 8, page 51, Nov. 1968.

44. Indian Standard Specification, IS : 648 - 1963.

45. T.D. Yensen, See N.P. Goss, Iron Age, 171, 147, Feb. 5, 1953.

46. A.A. Band, M. Tech. Thesis, Dept. of Metallurgical Engg., IIT, Kanpur, January 1972.

47. M.L. Narula, M.Tech. Thesis, Dept. of Metallurgical Engg., IIT, Kanpur, January 1972.

48. Hsun Hu, in "Recovery And Recrystallization Of Metals", Edited by L. Himmel; Gordon & Breach Science Publishers, N.Y., p. 311, 1962.

Fig. 1: Magnetization curve for pure Iron single Crystals.

Fig. 2: Magnetization curve for Iron + % silicon Single
Crystals.

Fig. 3: Planes and directions of cubic crystals that are
important for better magnetic properties in Fe and
Si-Fe alloys.

Fig. 4: Variation in saturation induction B_s, maximum
permeability μ_m, curie temperature Θ and
resistivity as a function of % Si in Fe.

Fig. 5: Hysteresis loss W_h, Coercive force H_C, Total loss
W_t and Maximum permeability μ_m as a function of Si
content for hot rolled commercial Si-Fe alloys.

Fig. 6: Tensile strength of Fe-Si alloys for different
concentrations of Si.

Fig. 7: Effect of Impurities on the change in Hysteresis
loss W_h (with respect to pure Fe) of 4% Si-Fe
alloy at B=10000 Gauss.

Fig. 8: Crystal orientation with respect to rolling plane
(the plane of the sheets) and the rolling directions
(R.D.) to give (a) cube texture, (b) cube-on-edge
texture (c) cold rolled texture.
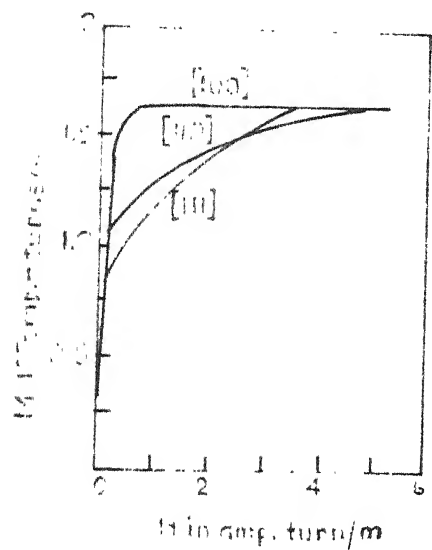
Fig. 1
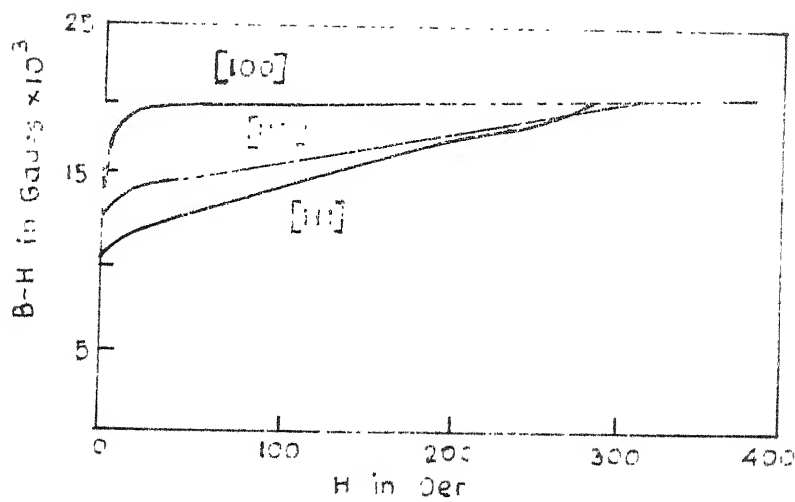
Fig. 2

Fig. 3

Fig. 8

Fig. 4

B_s, in Gauss & μ_m $\times 10^3$

θ, in C° & ρ, in Microhm – Cm $\times 10^2$

μ_m

B_s

θ

ρ

28
24
20
16
12
4

14
12
10
8
6
4
2

0   2   4   6   8   10

% Si

Fig. 4

Fig. 6

T.S in Psi $\times 10^4$

10^4

8
4

0   2   4   6

% Si

Fig. 6

Fig. 7

W_h, in Ergs /Cm^3/Cy.

C
S
O
Mn
P

12
8
4
0
-4

0   0.04   0.08   0.12

% Element

Fig. 7

Fig. 5

W_h, in Ergs /Cm^3/ Cy.

$\mu_m \times 10^4$, H_c in Oer., W_t in W/lb

$10^3 \times 2.4$

$B_m = 10^4$ Gauss

Wh
Wt
Hc
μm

2.4
2.0
1.6
1.2
0.8
0.4
0

1   2   3   4

% Si
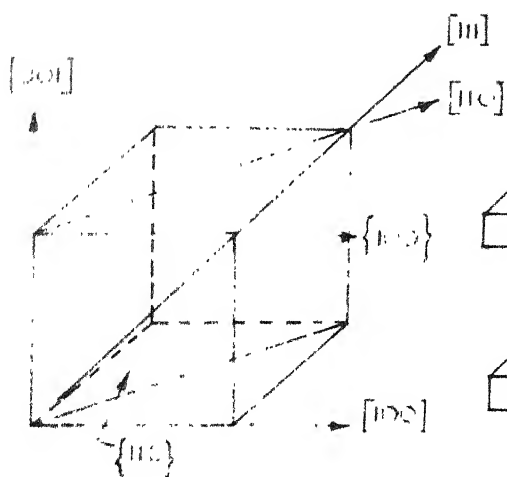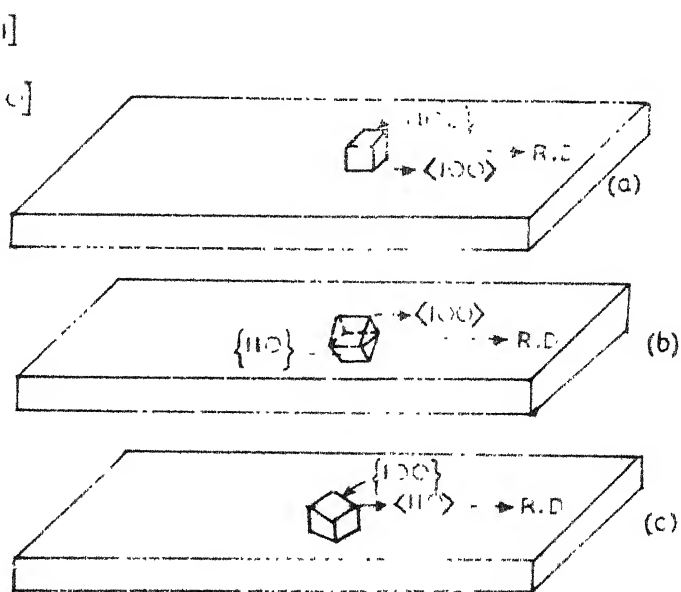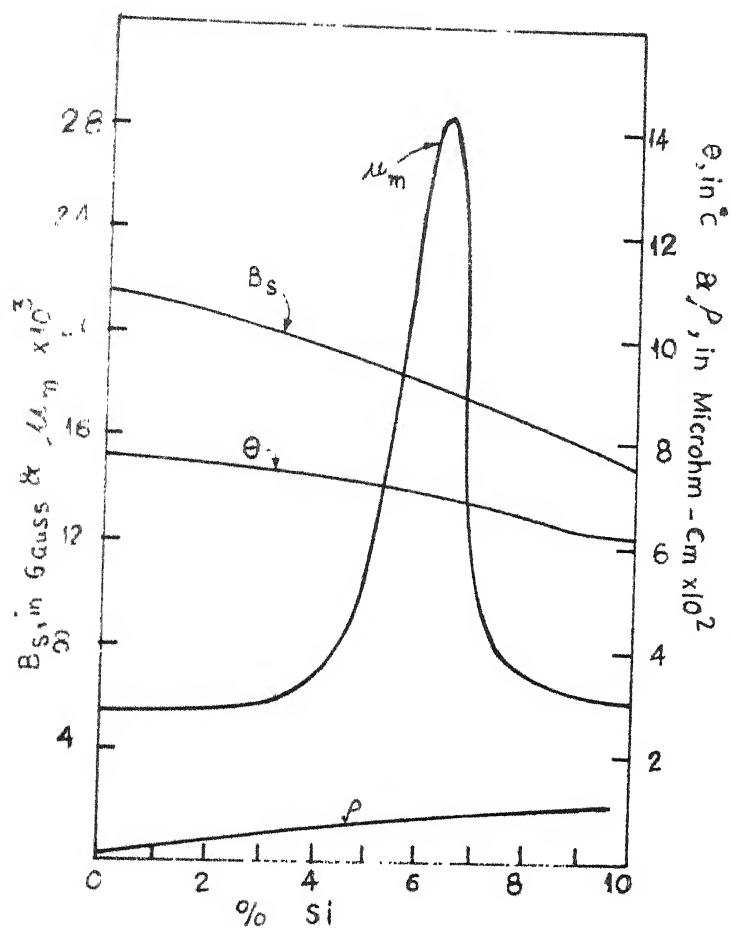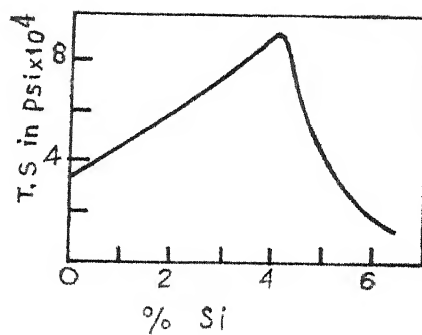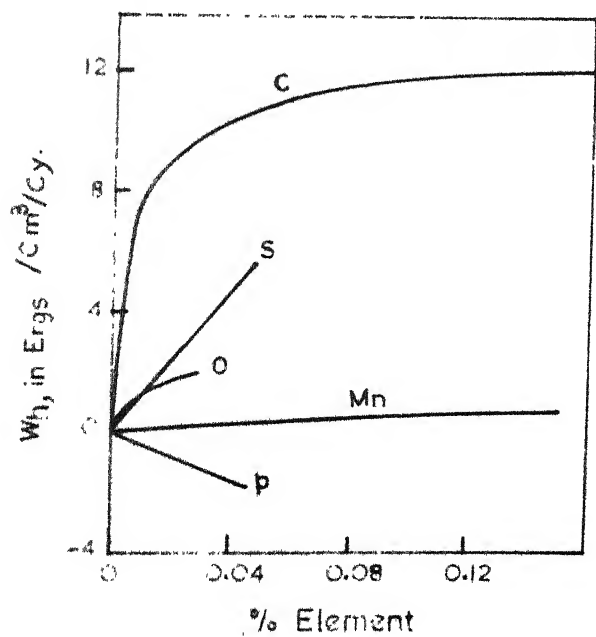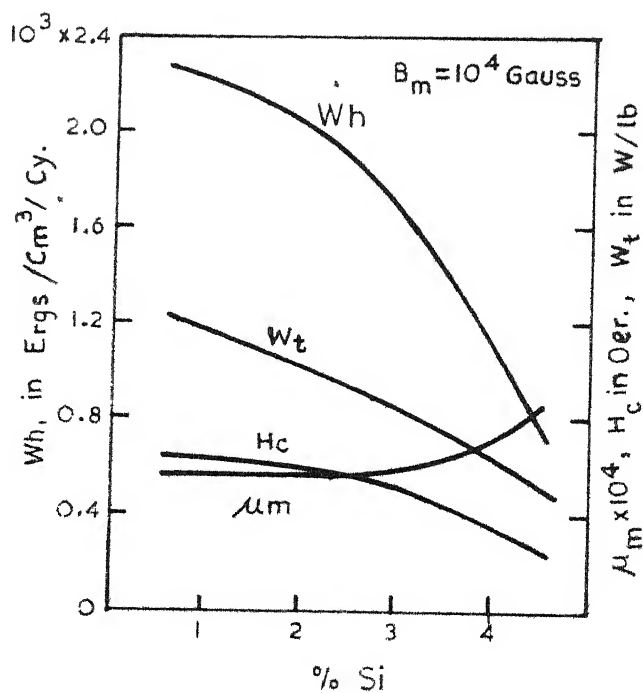
Fig. 5

Fig. 9. Epstein Test Frame

EPSTEIN TEST FRAME
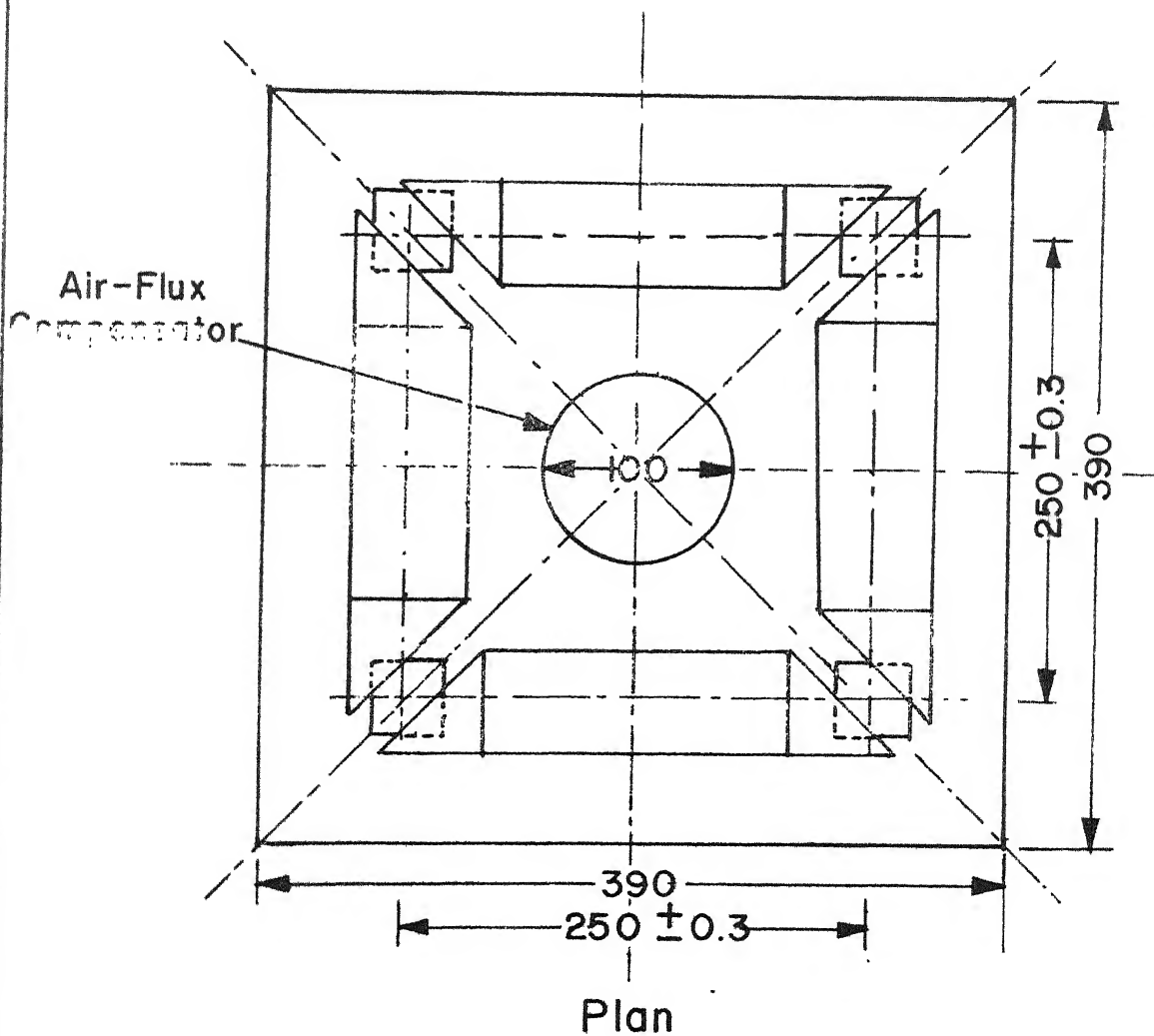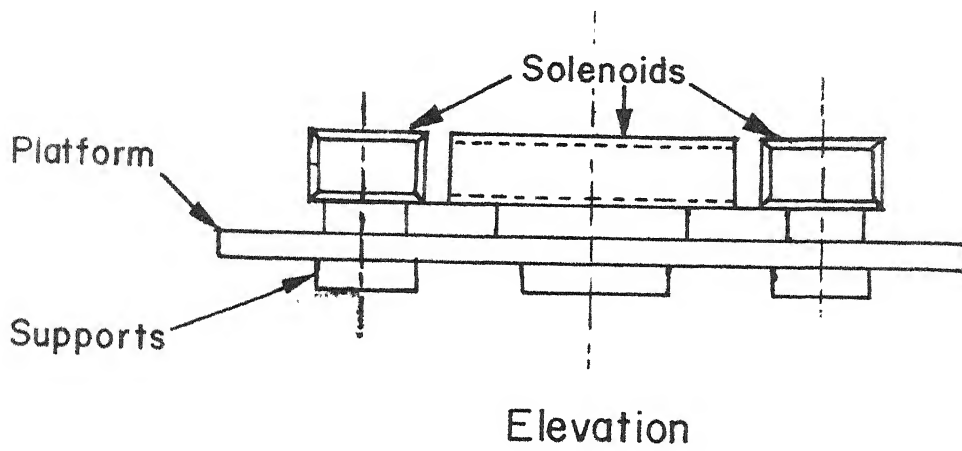
Elevation

Plan

Dimensions in mm.

CIRCUIT DIAGRAM

FIG. 10

MODIFIED CIRCUIT DIAGRAM

FIG.11
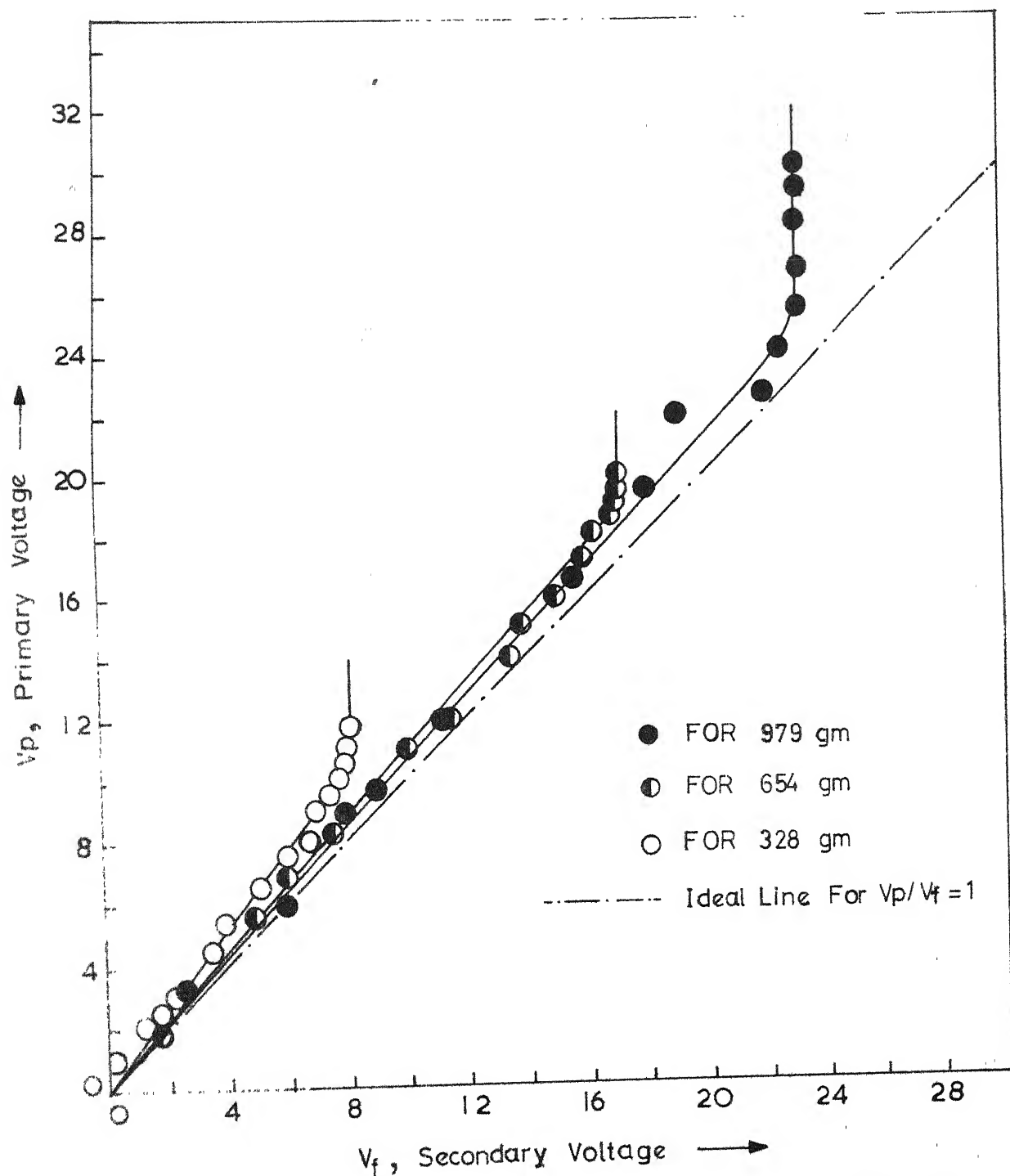
FIG 12 RELATION BETWEEN THE APPLIED AND INDUCED VOLTAGES
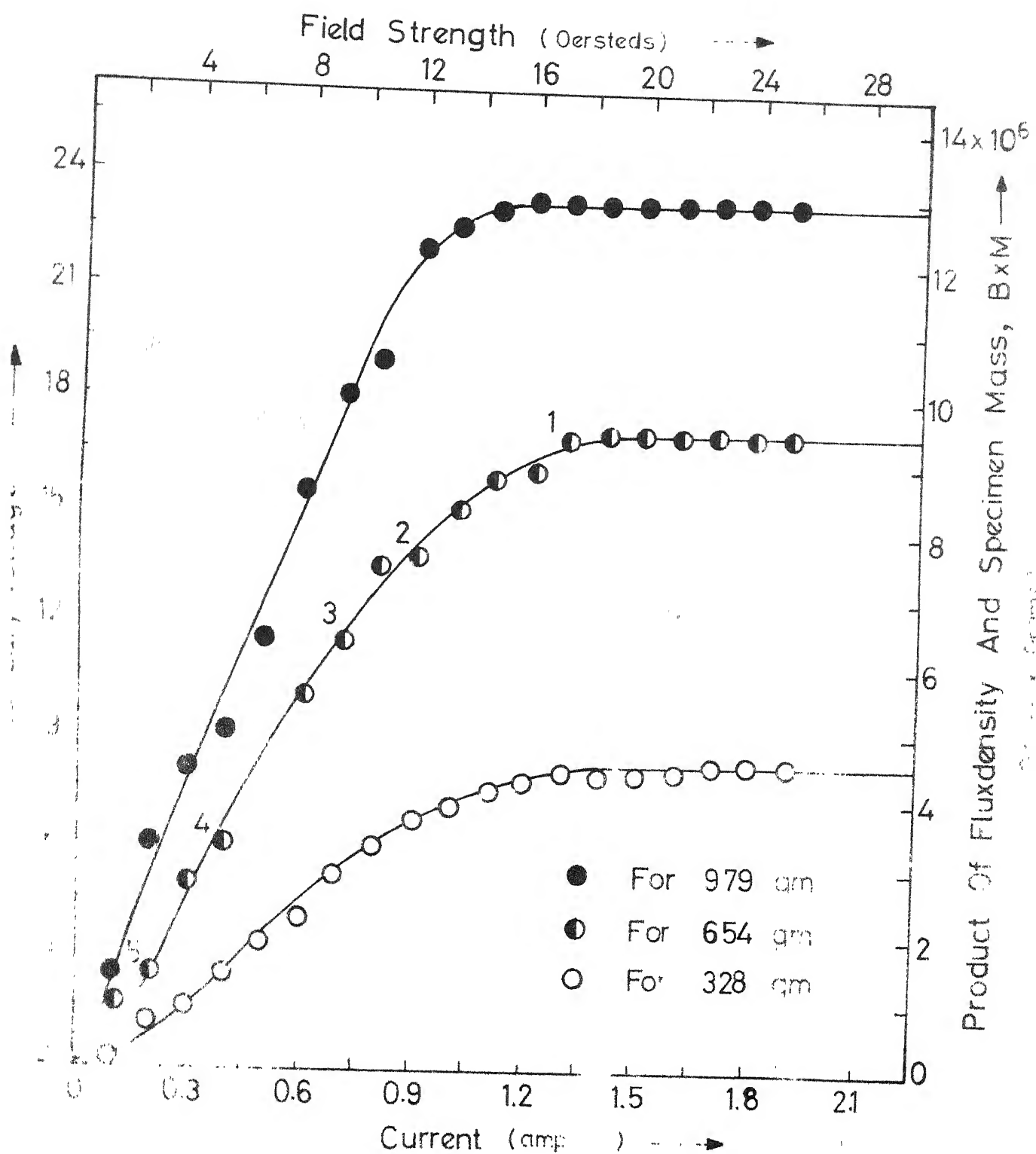
Fig. 13 Variation Of Secondary Voltage With Applied Current For Different Specimen Masses Of Mild Steel
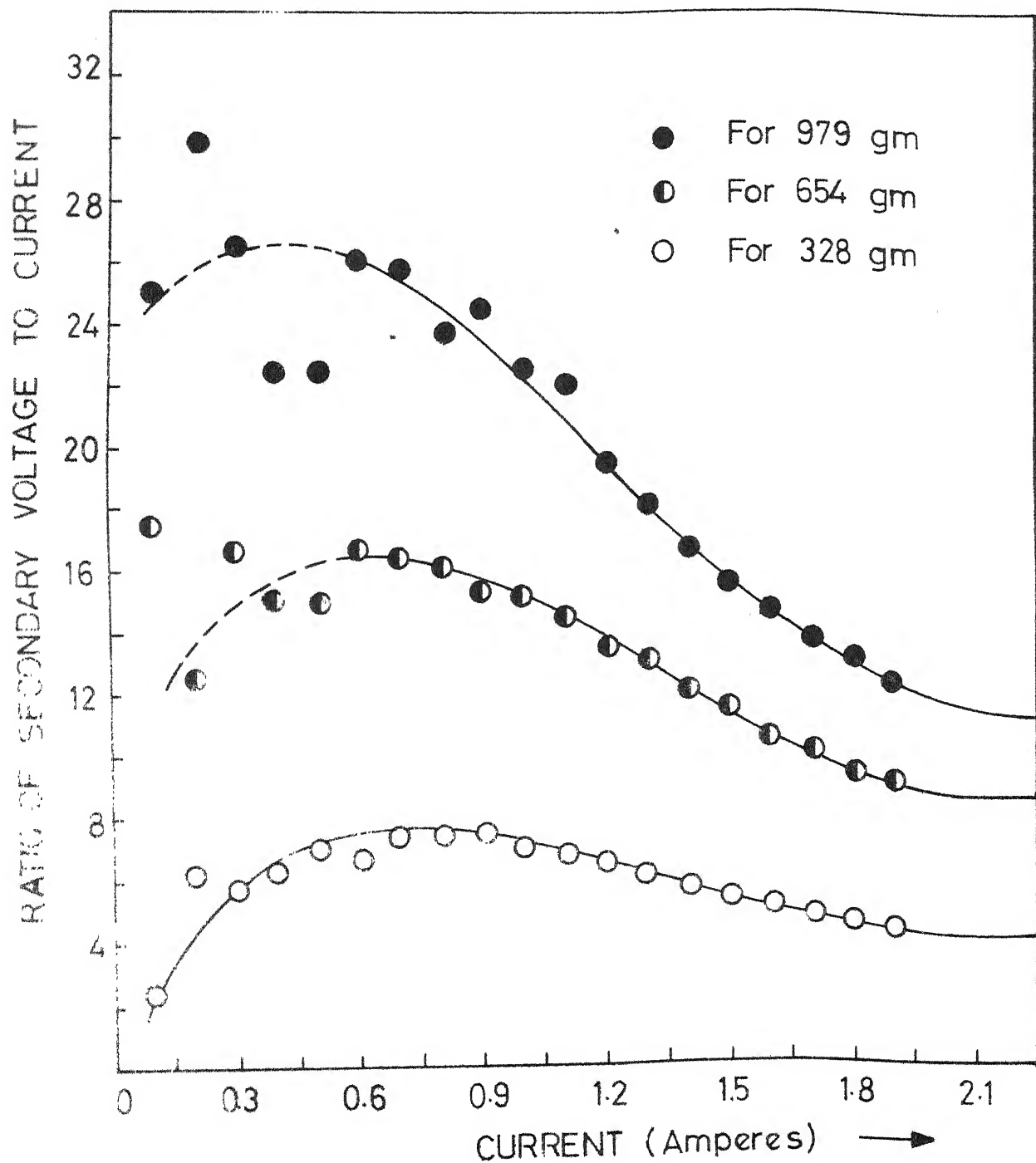
FIG. 14.
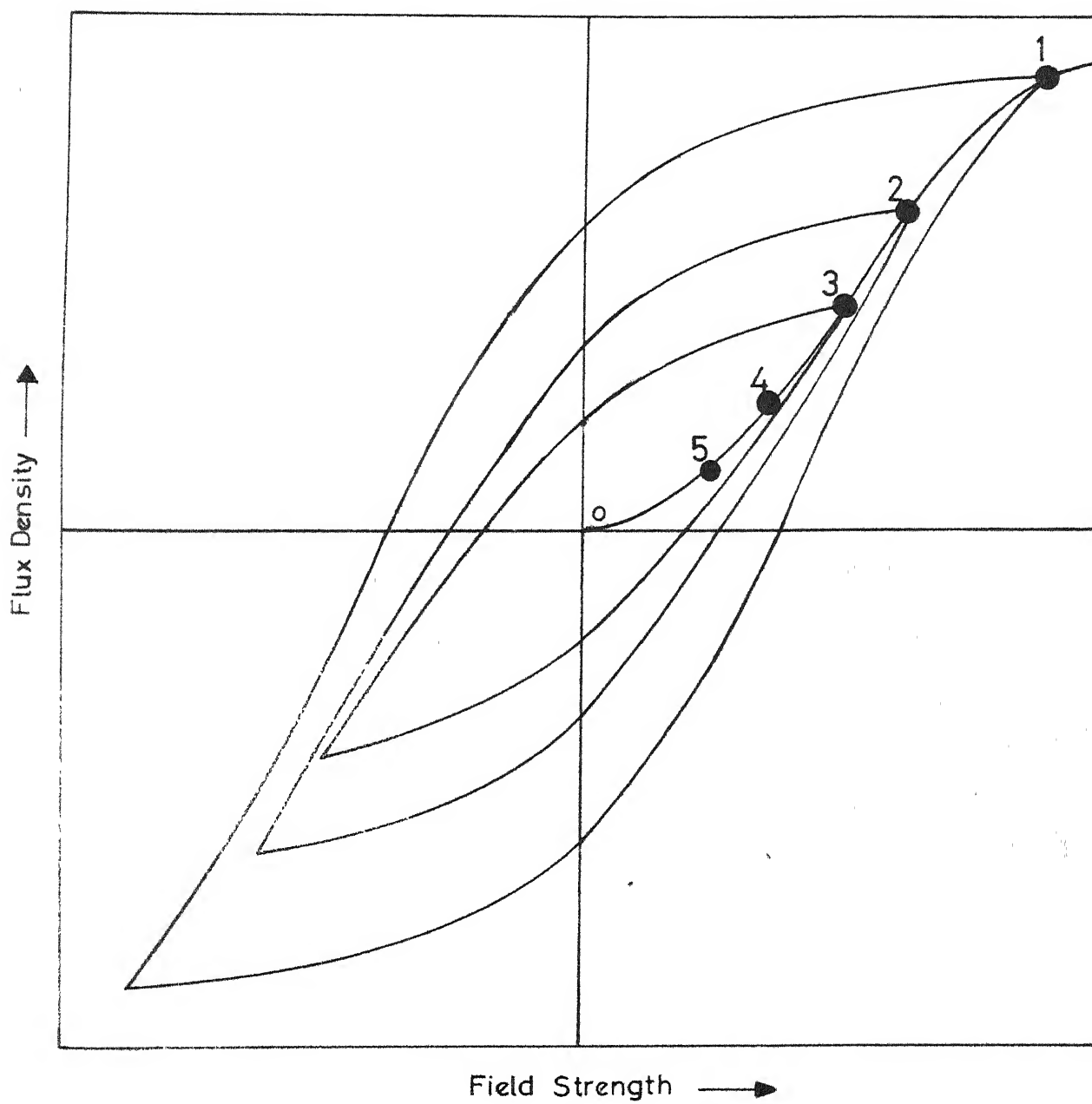
FIG.15   Schematic   Sketch   Of   Hysteresis   Loops
(Refer Fig.13)

Fig. 16   Controlled atmosphere high frequency induction melting furnace.

Fig. 17   Gas purification train & heat treatment furnace interconnection.

TO

n Gas (Purified)

TO Vacuum Gauge

109

COOLING COIL

VYCOR TUBE

TO Vacuum Pump

GRAPHITE SUCCEPTOR

INDUCTION COIL

CRUCIBLE

REFRACTORY SLEEVES

Dimensions in mm

To Melting Unit

P_2O_5

$CaCl_2$

Heat Treatment Furance

Cu

Tl

$CaCl_2$

From Argon-Gas Cylinder.

Oil
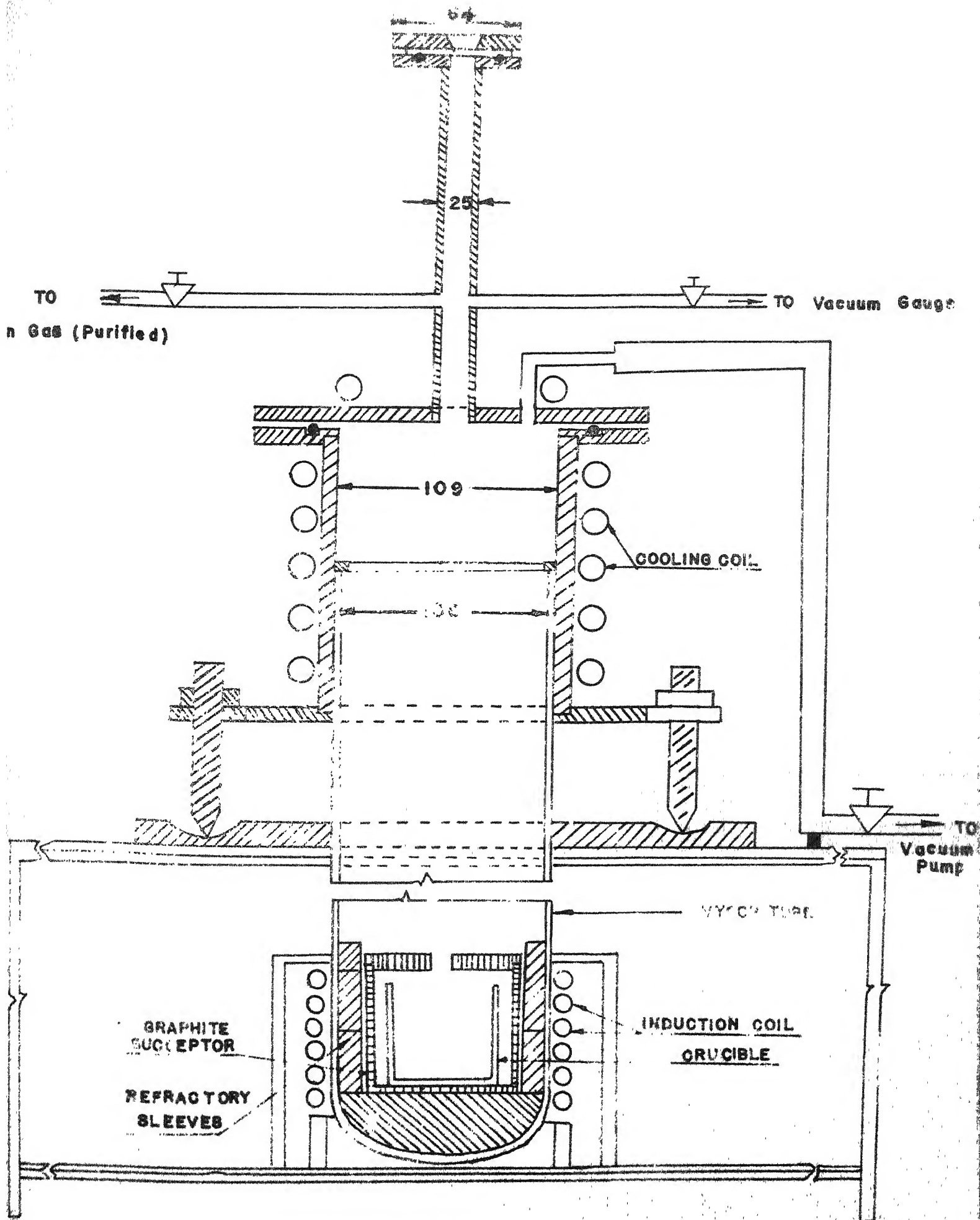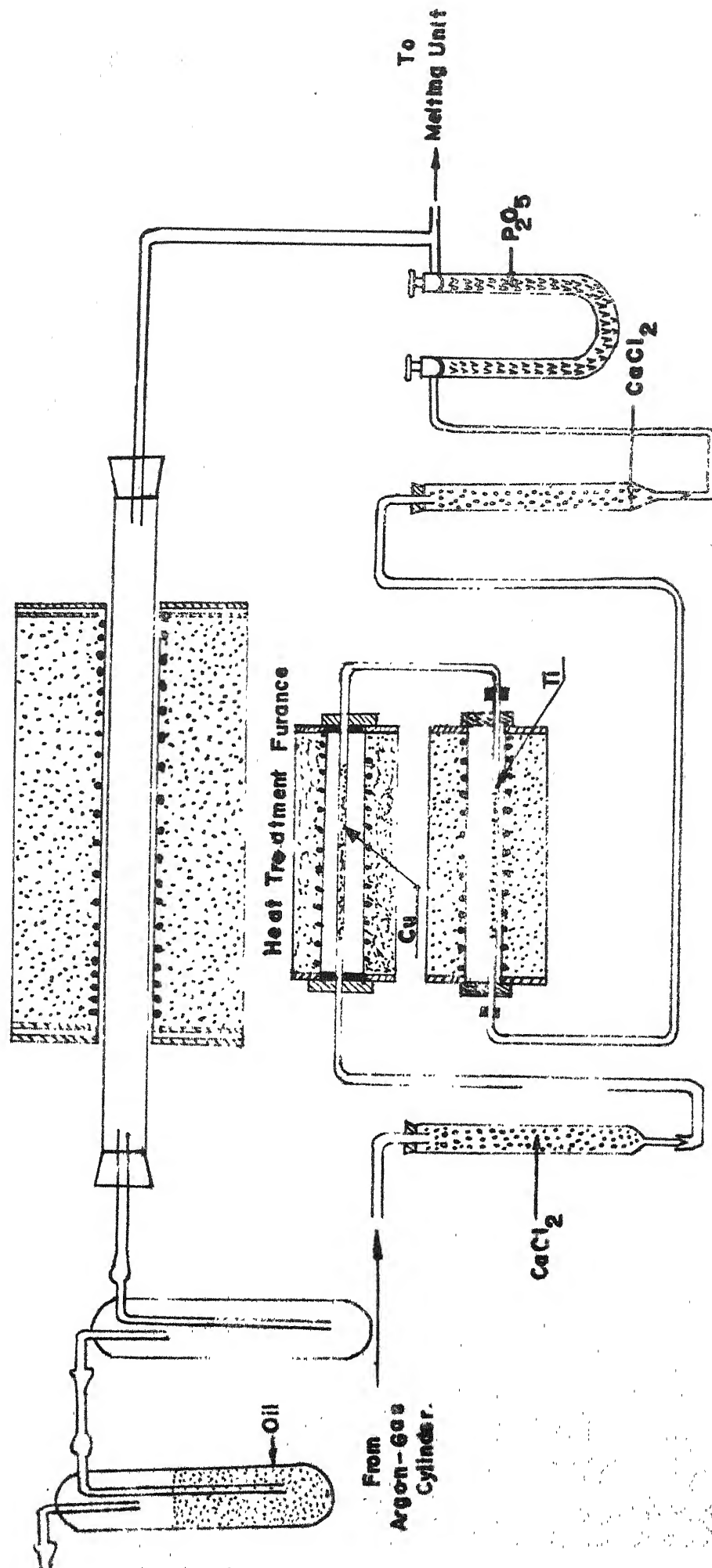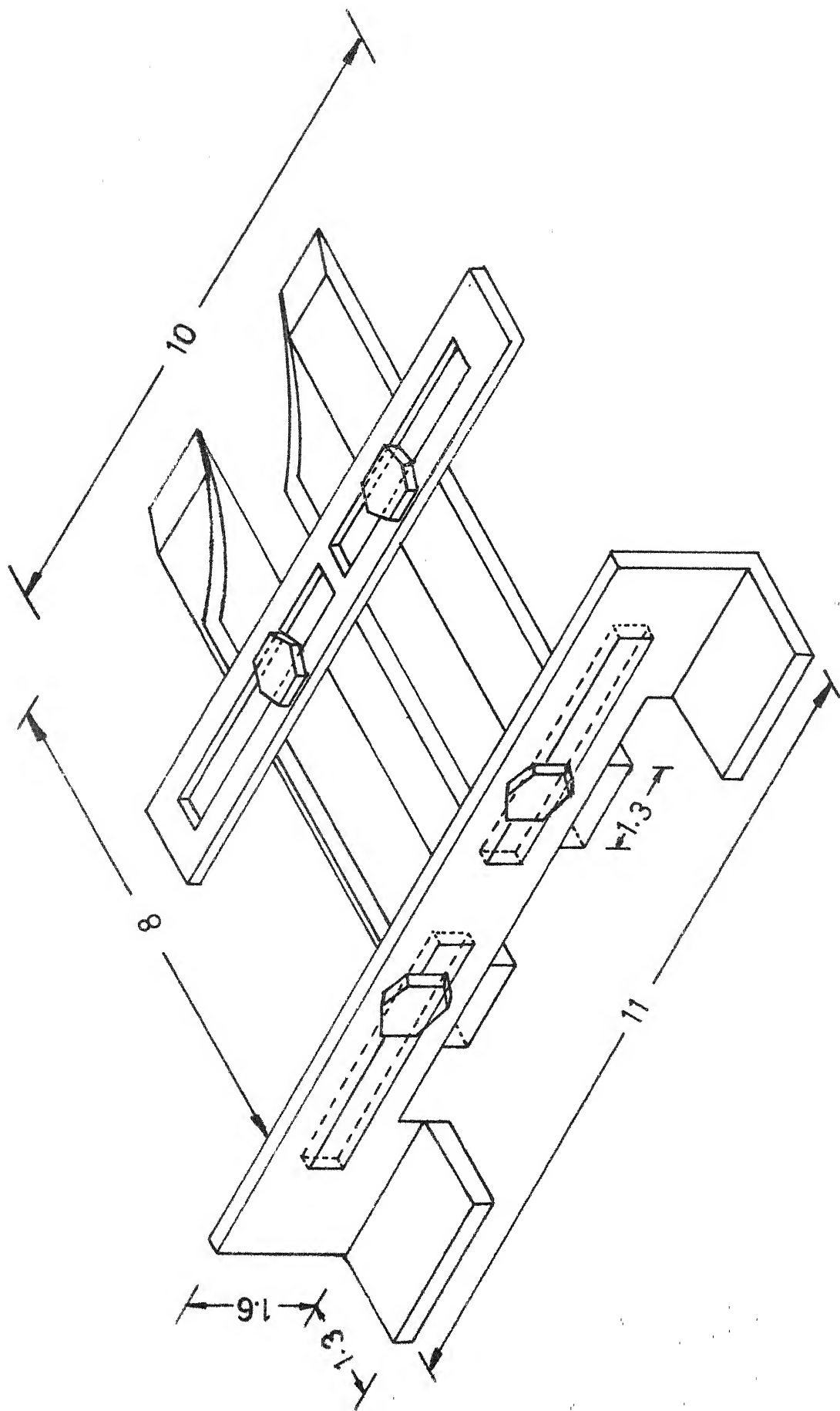
FIG   ISOMETRIC   VIEW   OF   THE   GUIDE

Dimensions   In   Inches
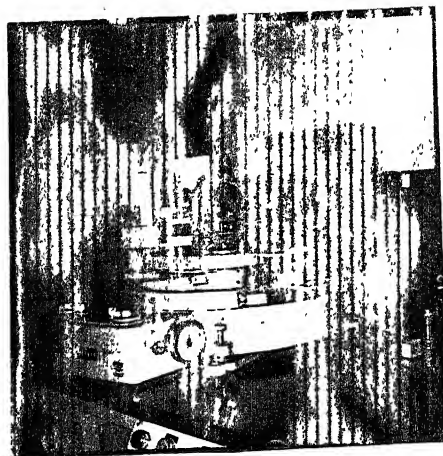
Fig. 20   Transmission Goniometer fitted on Diffractometer.
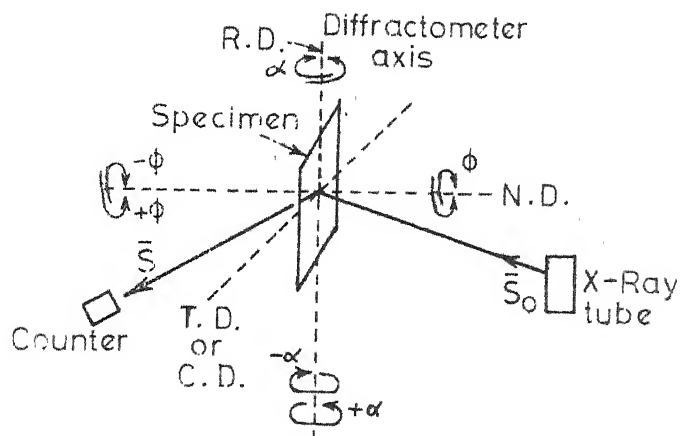
Fig.   Diffractometer geometry for transmission
technique. The positions of rolling direction
(R.D.) Transverse or cross direction (T.D. or C.D.)
and normal direction (N.D.) correspond to
$\alpha = 0$ and $\phi = 0$

R.D.

T.D.

SHEET
NORMAL

$+\phi$

Reflecting
plane
normal

$-\alpha$

(b)
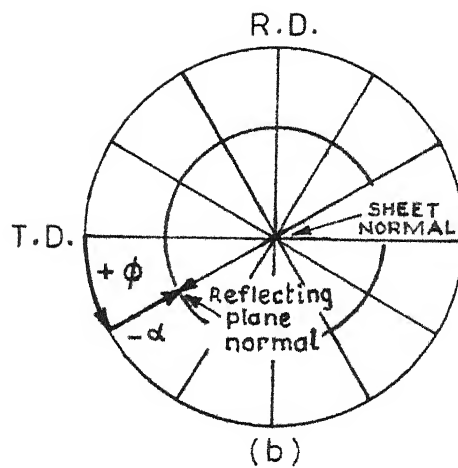
Fig.   Angular relationships in the tranmission pole
figure method on the stereographic projection
(On the projection the position of the reflecting
plane normal is shown for $\phi = 30°$ and $\alpha = -30°$)

Location of [1̄10] poles in

(130)	Projection ⊙
(110)	Projection ·
(211)	Projection ×
(111)	Projection ○
(001)	Projection □

--- Rolling and transverse
directions for (001) [1̄10]
texture (cold rolled texture)

— Rolling and transverse
direction for a (011) [1̄00]
texture (cube on edge texture
and (b) (001) [1̄0̄0] texture
(cube texture)
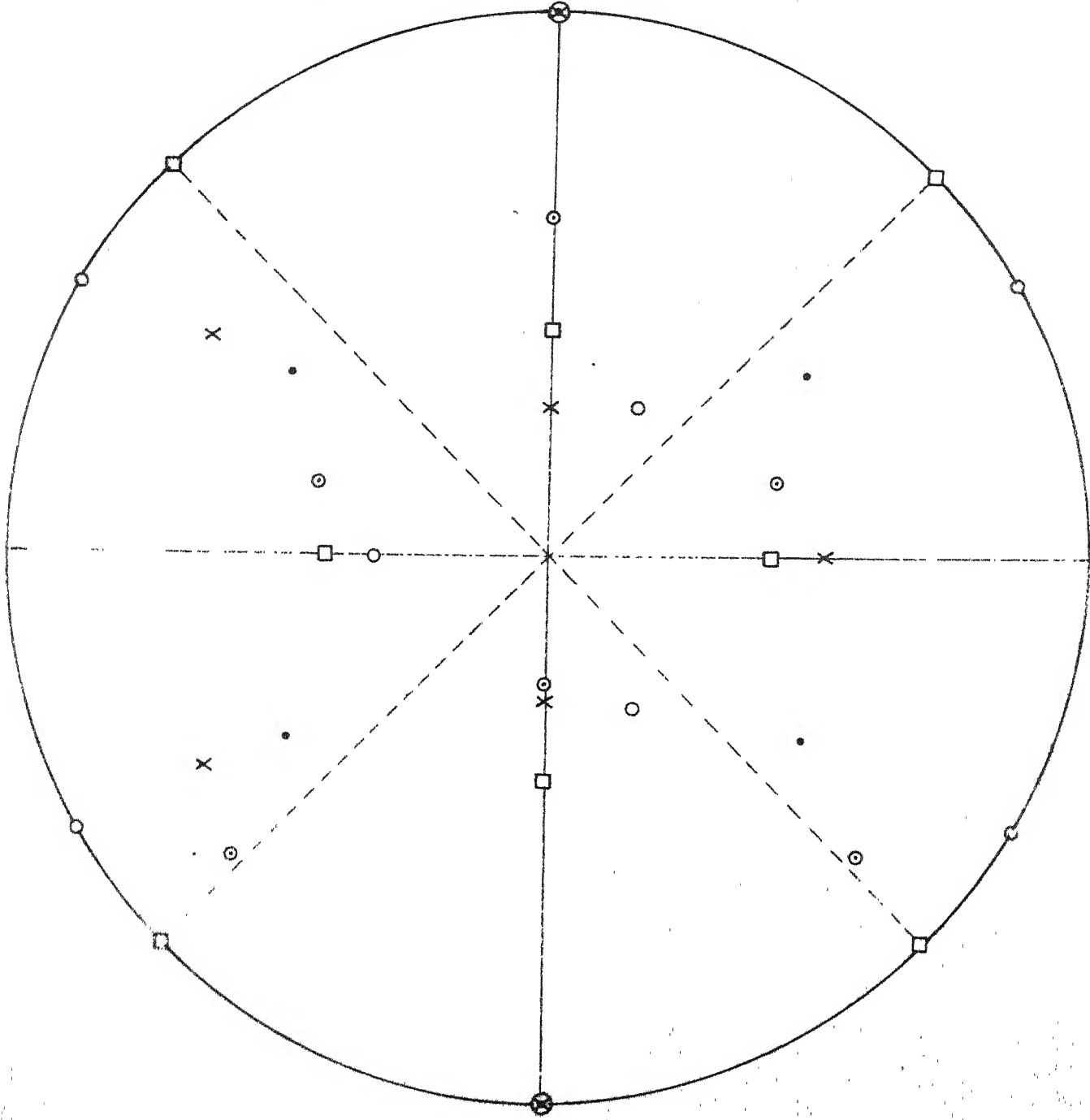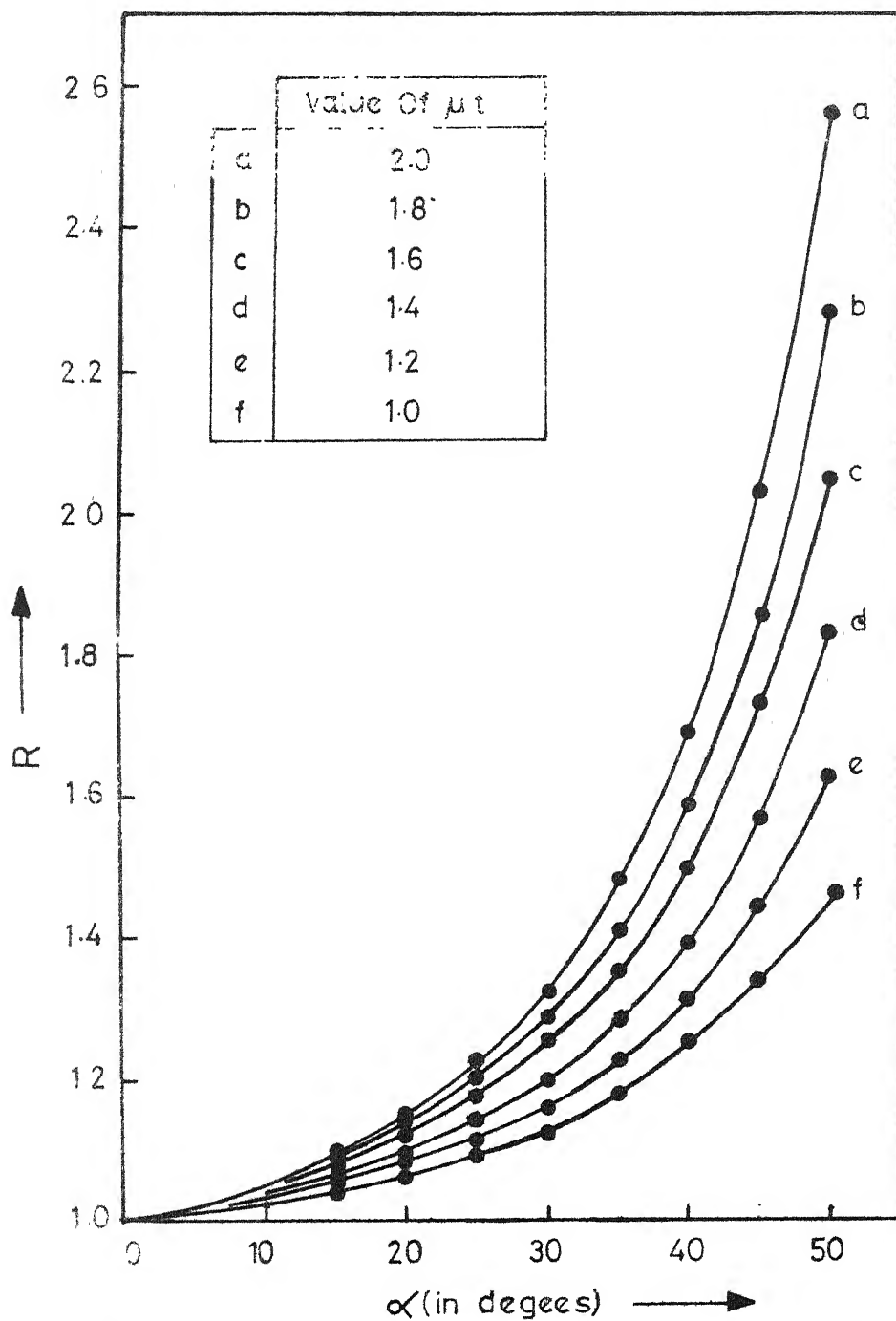
	Value Of μt
a	2.0
b	1.8
c	1.6
d	1.4
e	1.2
f	1.0

FIG a. Correction Factor R As Function Of α For Constant Value Of μt

	Value Of μt
a	1.9
b	1.7
c	1.5
d	1.3
e	1.1

FIG b. Correction Factor R As Function
Of α For Constant Value Of μt
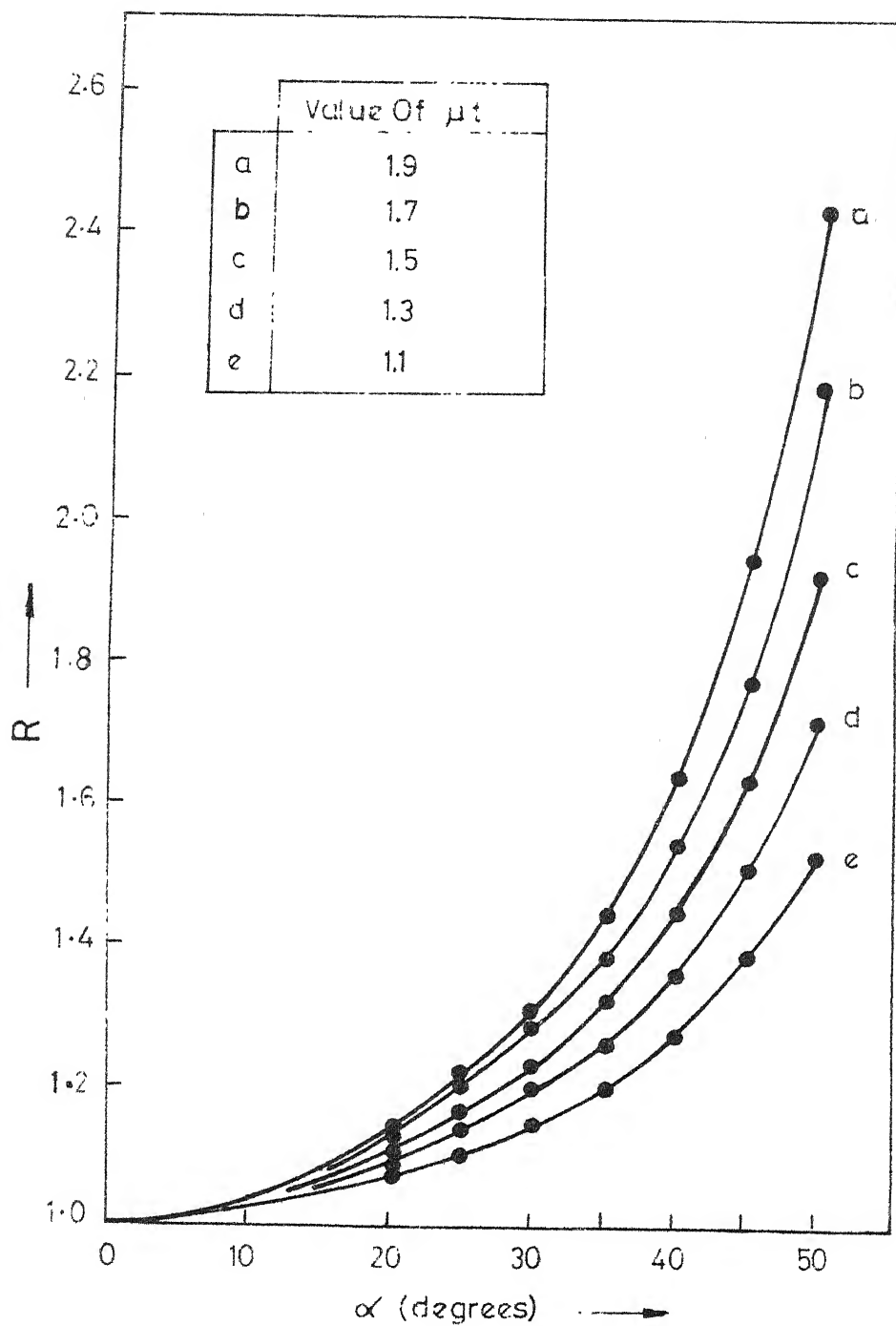
	Value Of α
a	$-50°$
b	$-45°$
c	$-40°$
d	$-35°$
e	$-30°$
f	$-25°$
g	$-20°$
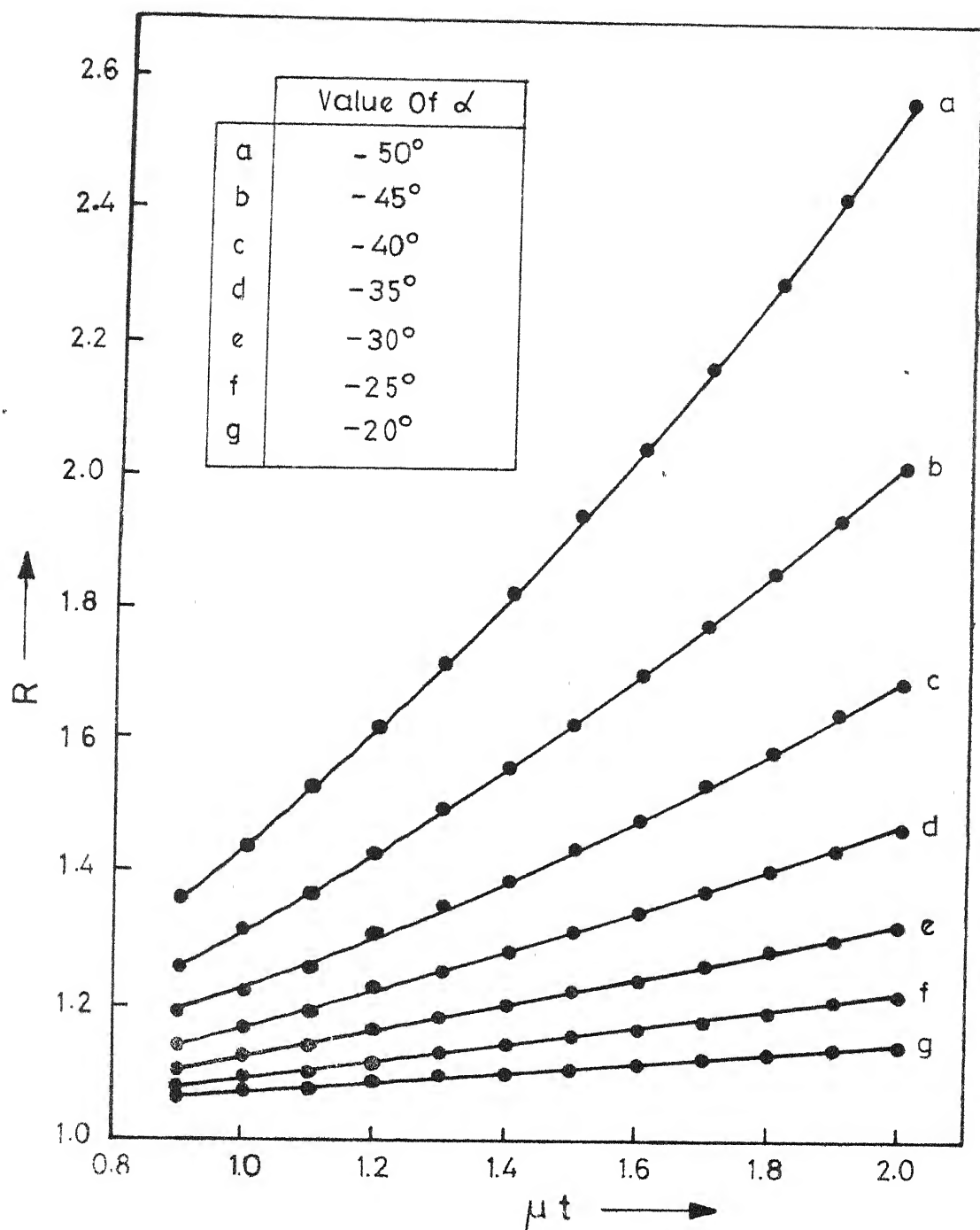
FIG . Correction Factor R As Function
Of μt For Constant Value Of α

Fig. 26: Fe-Si phase diagram

Fig. 27: Modification of Fe-Si Diagram with variation in

Carbon concentration.

Fig.

% Si

Temp. in °C × 100

α

α+γ(·07%C)
α+γ (·01%C)
α+γ+Carbide(·07%C)
α+Carbide

γ

14 12 10 8 6

6 5 4 3 2 1 0

Fig.

At % Si

Temp. in °C × 100

ε+η
ε+θ
ε
α'+ε
α"+η
η+ε
α+η
α+ε
α+η
α+α'
α+η
α
α+γ
α+γ

0 20 40 60
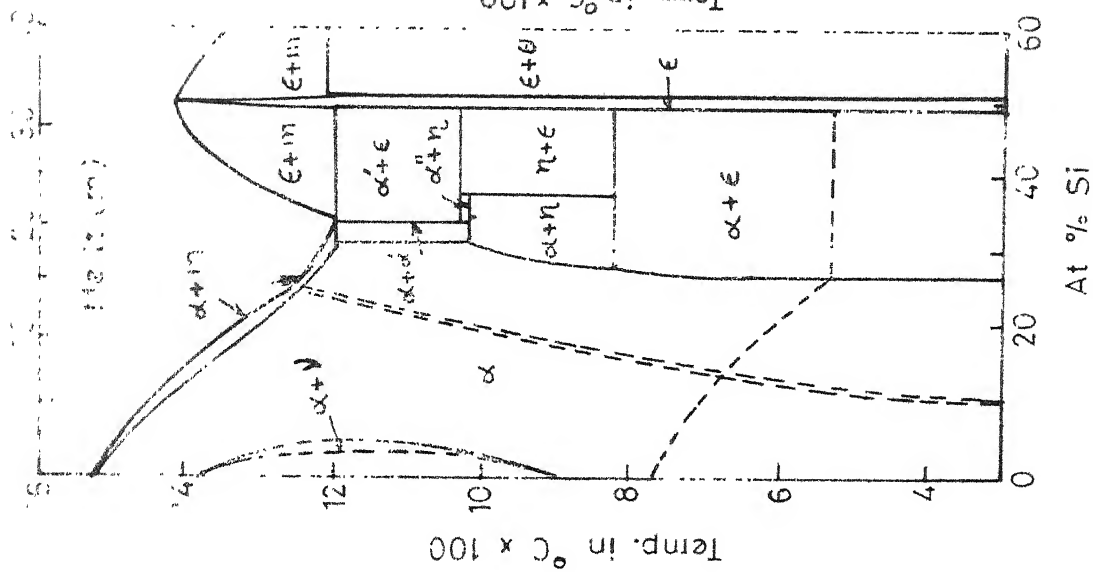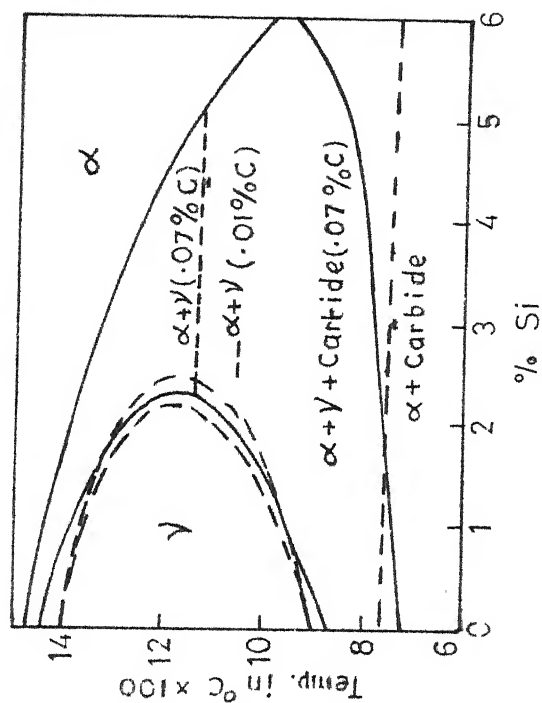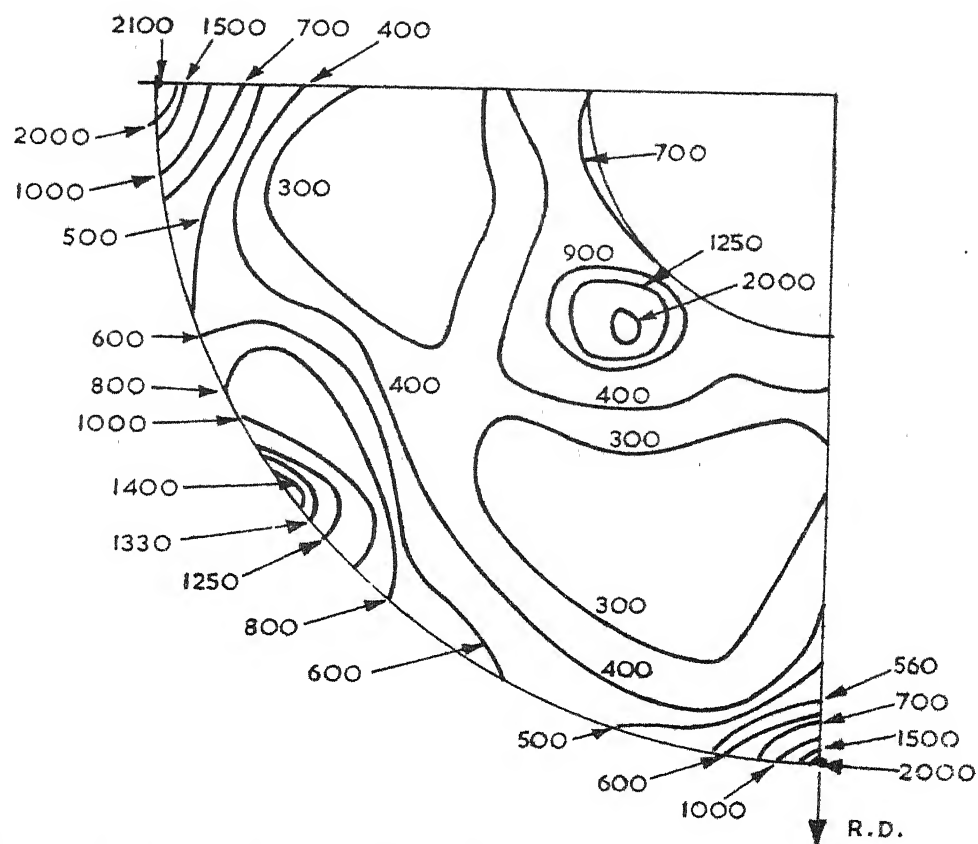
Fig. 28   Specimen G, 3% Si-Fe alloy
          alternate   C.R.
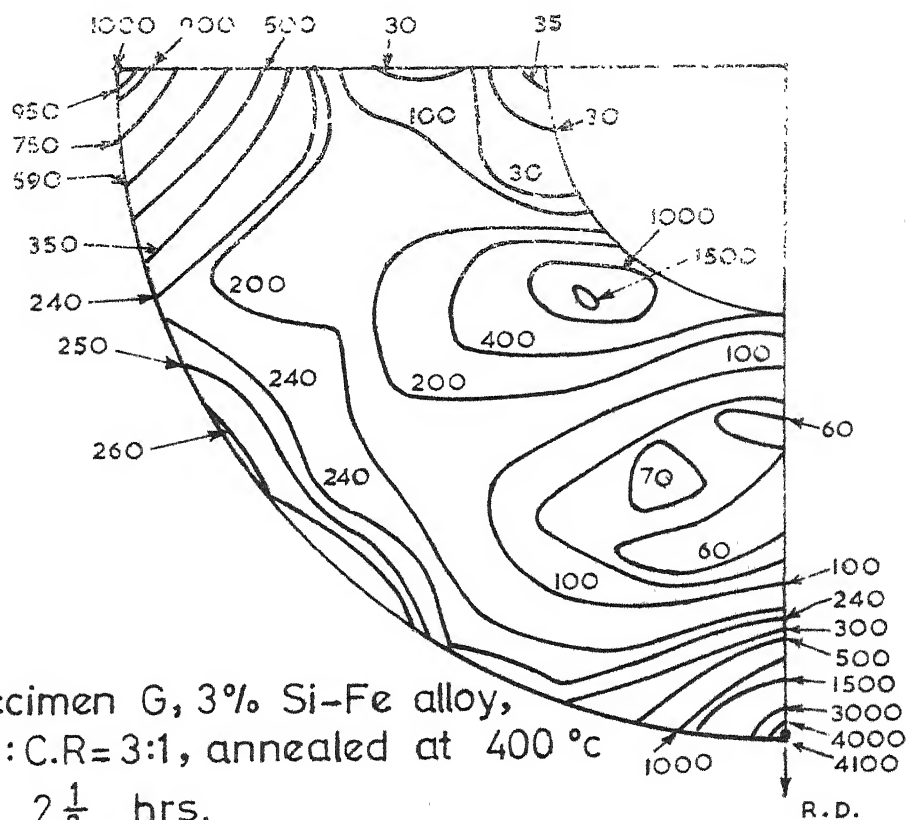
Fig. 30   Specimen G, 3% Si–Fe alloy,
S.R : C.R = 3:1, annealed at 400 °c
for 2½ hrs.
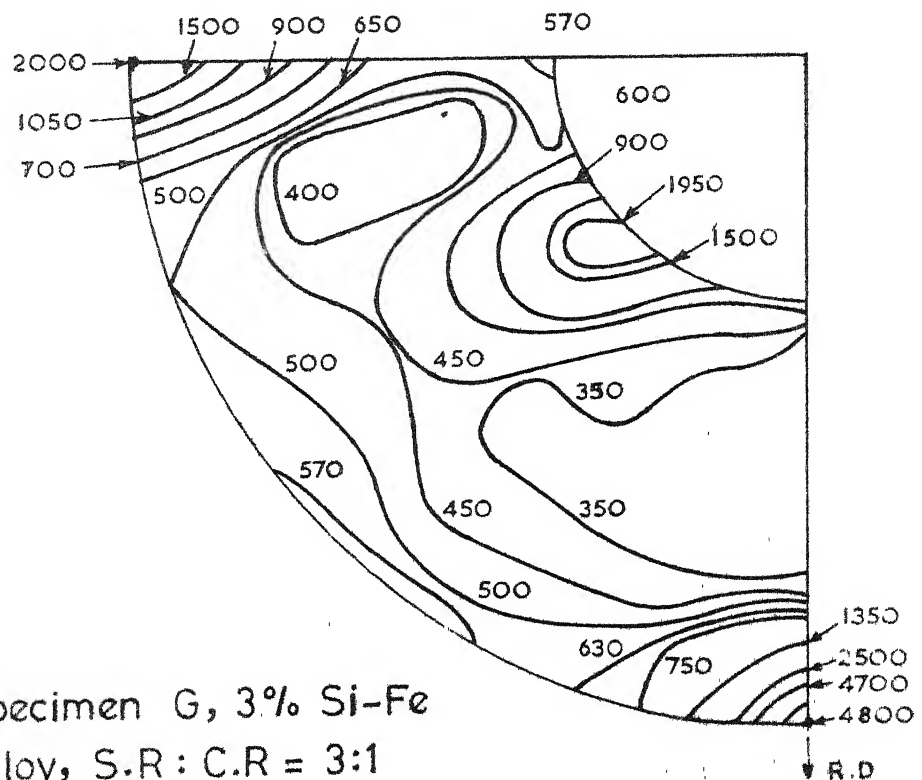
Fig. 29   Specimen G, 3% Si–Fe
alloy, S.R : C.R = 3:1
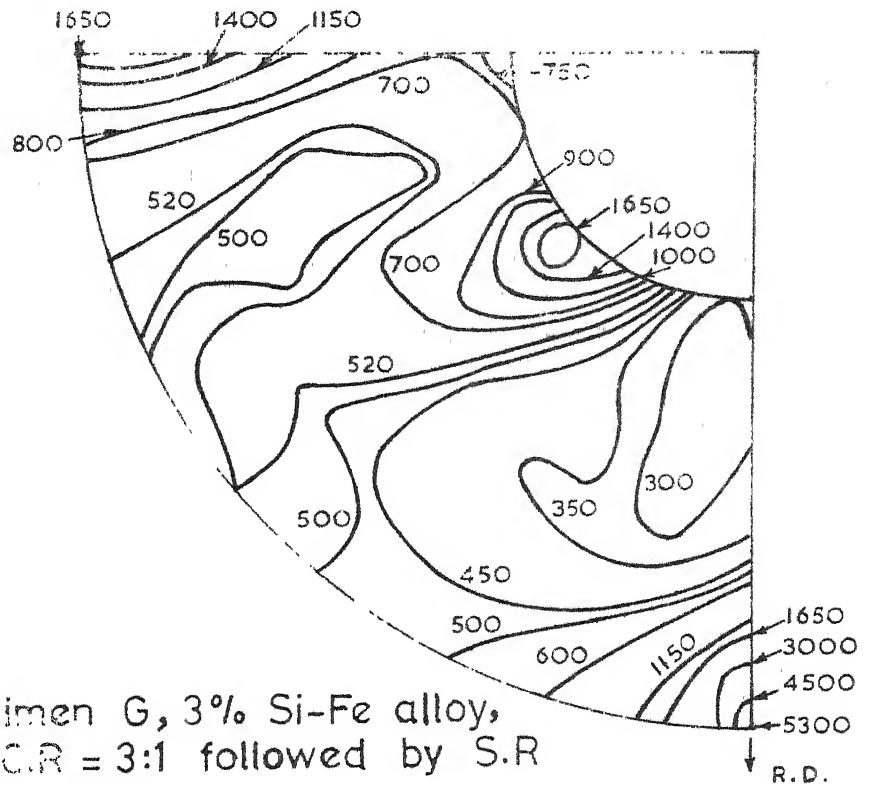
Fig. 31   Specimen G, 3% Si-Fe alloy,
           S.R·C.R = 3:1 followed by S.R
           to final thickness.
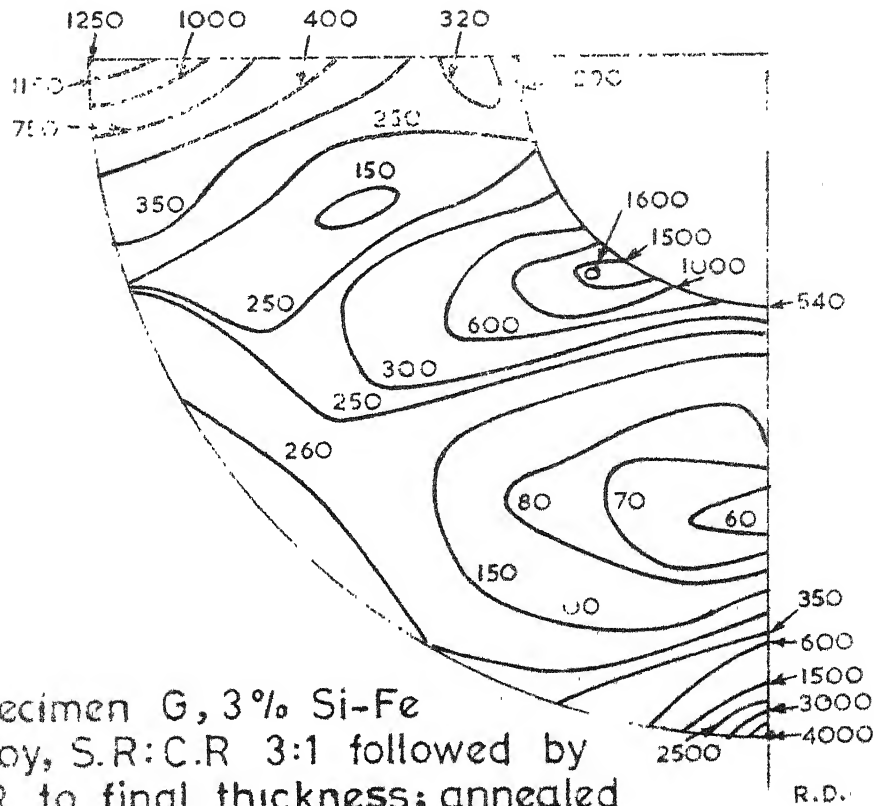
Fig. 32   Specimen G, 3% Si-Fe
           alloy, S.R:C.R 3:1 followed by
           S R to final thickness; annealed
           at 400 °c for $2\frac{1}{2}$ hrs.
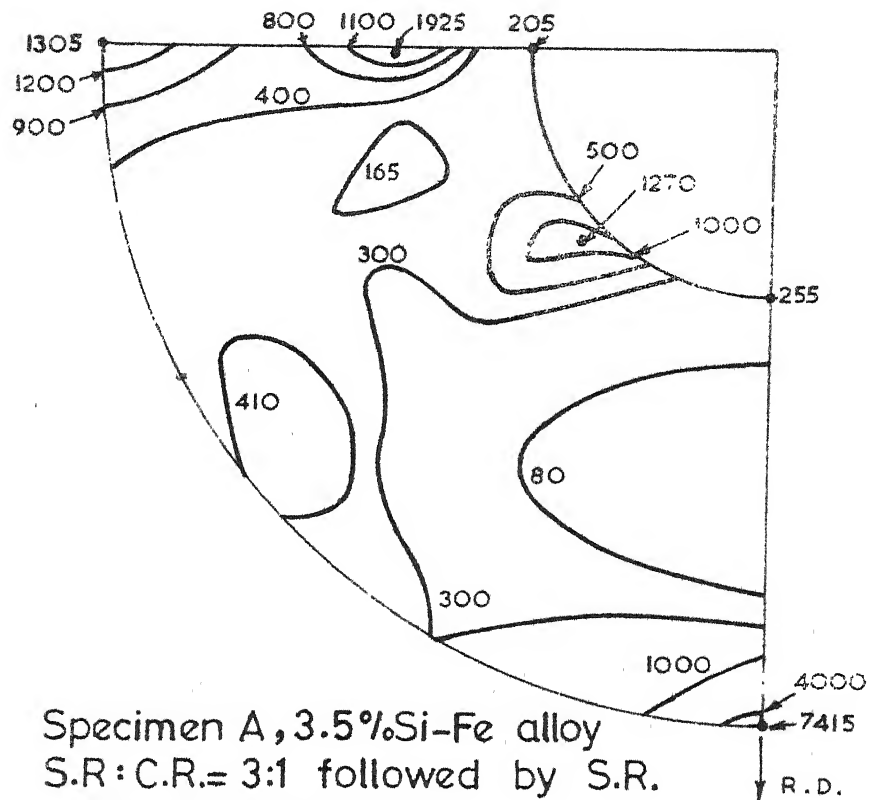
Fig. 35   Specimen A, 3.5% Si-Fe alloy
S.R : C.R. = 3:1 followed by S.R.
to final thickness.
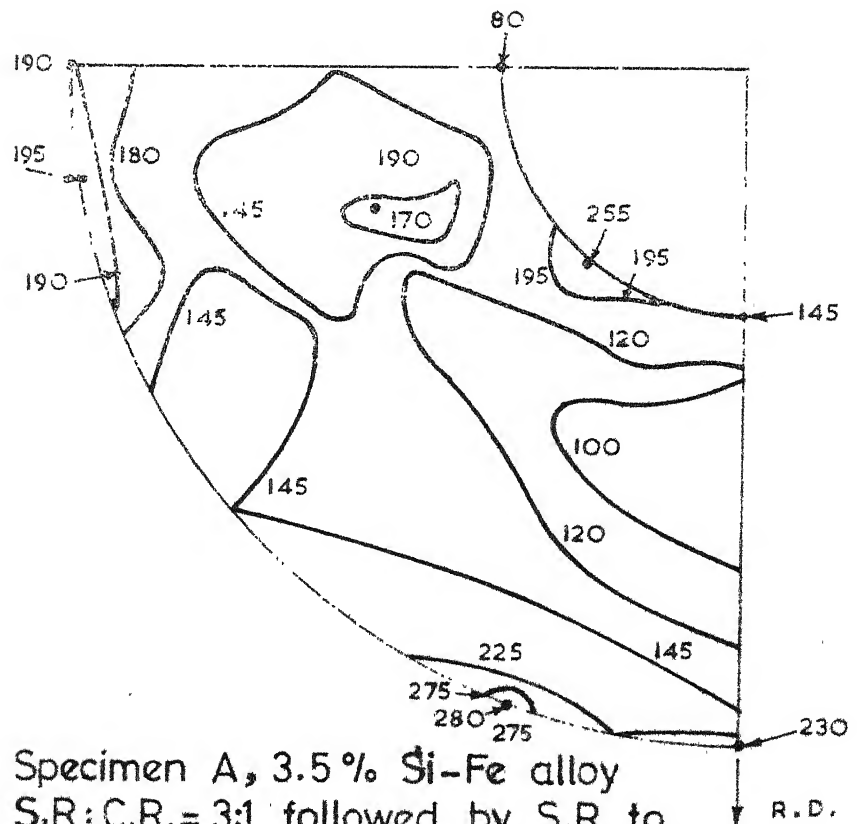
Fig. 36   Specimen A, 3.5% Si-Fe alloy
S.R : C.R. = 3:1 followed by S.R. to
final thickness annealed at 550°c
for 1/2 hrs.

Fig. 37   Specimen E_{comm}, 3% Si-Fe
          alloy, alternate cross rolled.

Fig. 38   Specimen E_{comm}, 3% Si-Fe
          alloy, alternate cross rolled,
          annealed at 400°c $2\frac{1}{2}$ hrs.
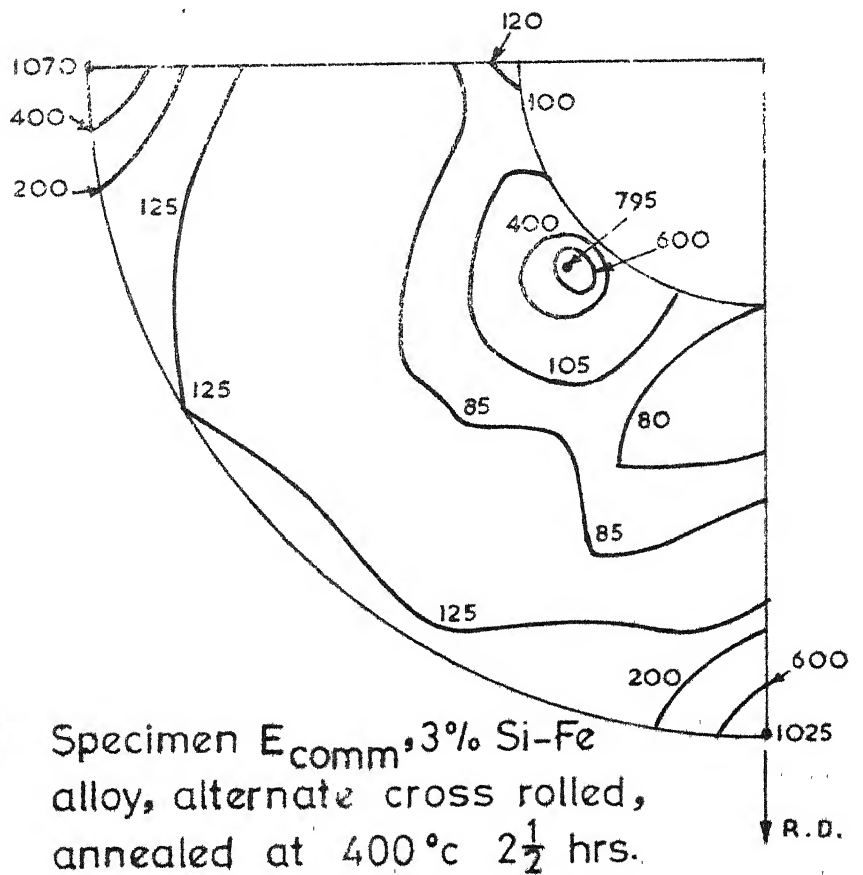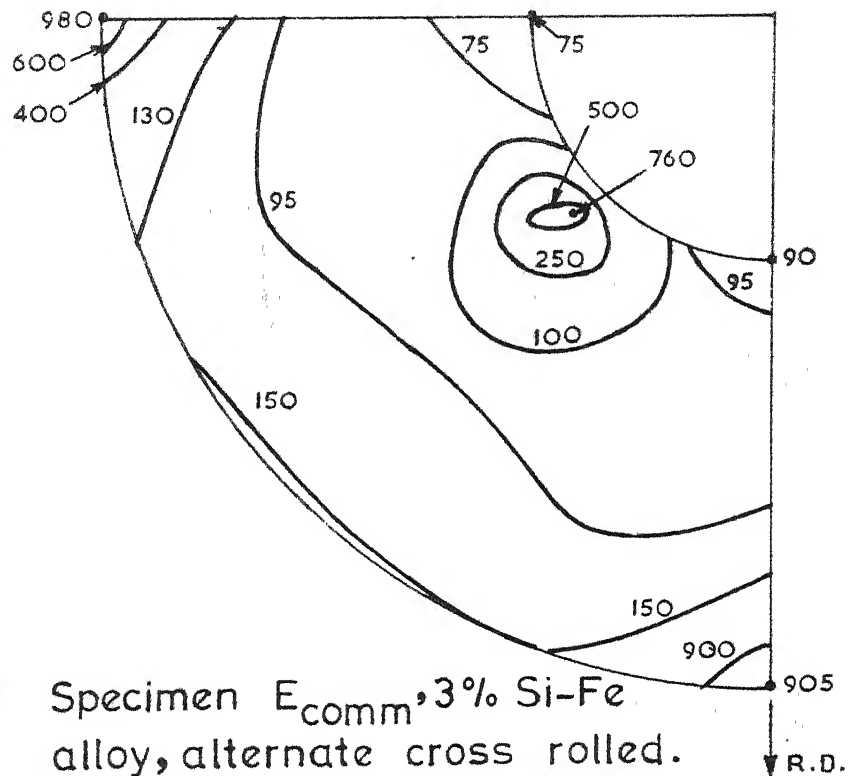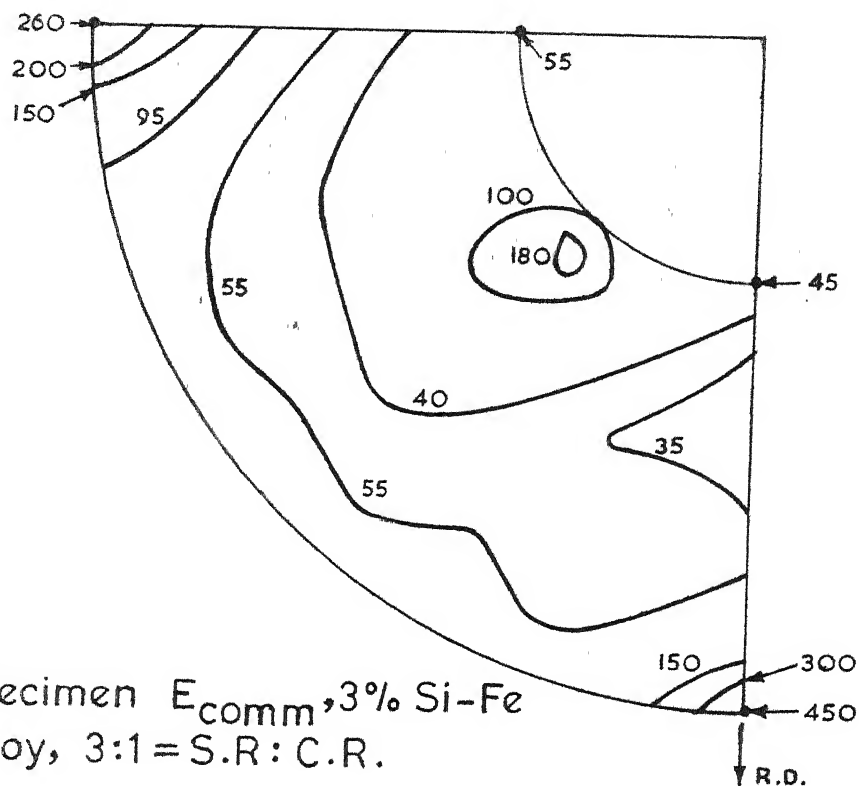
Fig. 39 Specimen E_{comm}, 3% Si-Fe
alloy, 3:1 = S.R : C.R.
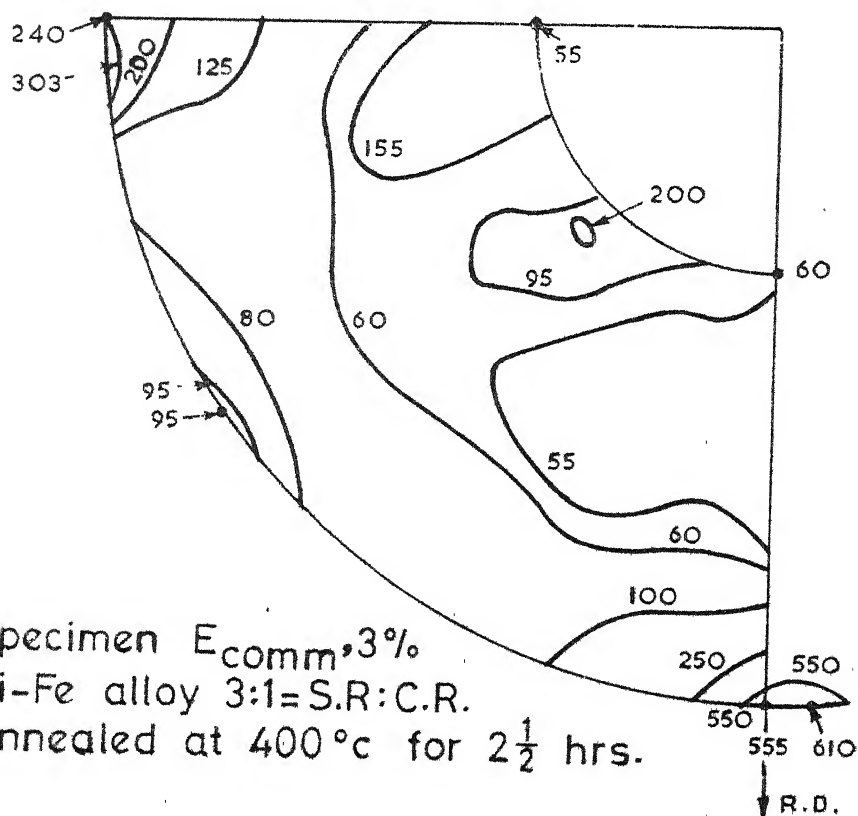
Fig. 40 Specimen E_{comm}, 3%
Si-Fe alloy 3:1 = S.R : C.R.
annealed at 400°c for $2\frac{1}{2}$ hrs.
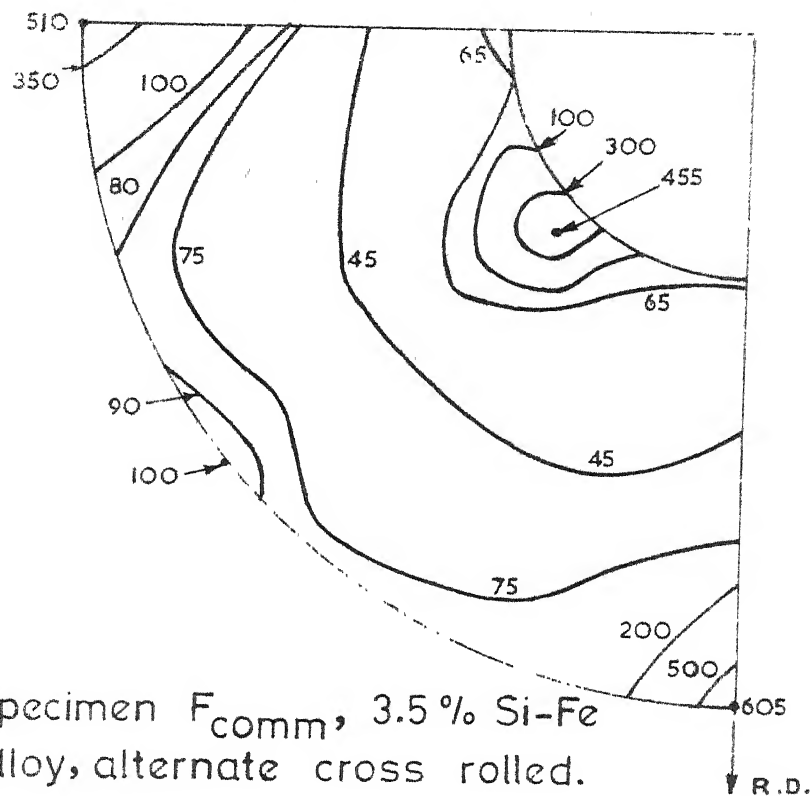
Fig. 41   Specimen F$_{comm}$, 3.5% Si–Fe
alloy, alternate cross rolled.
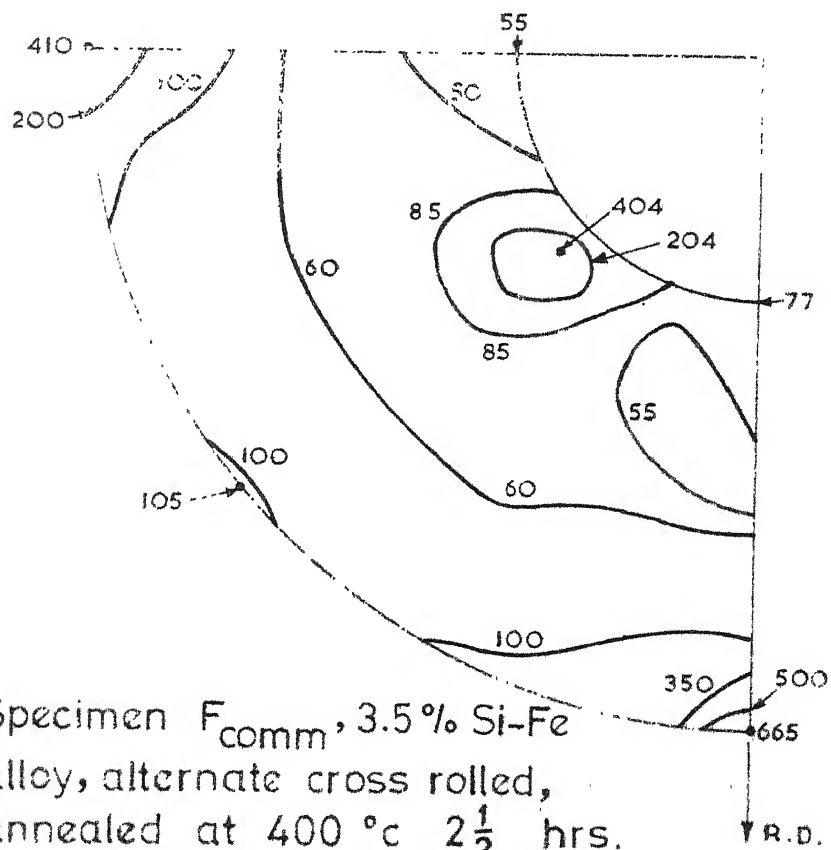
Fig. 42   Specimen F$_{comm}$, 3.5% Si–Fe
alloy, alternate cross rolled,
annealed at 400 °c 2$\frac{1}{2}$ hrs.
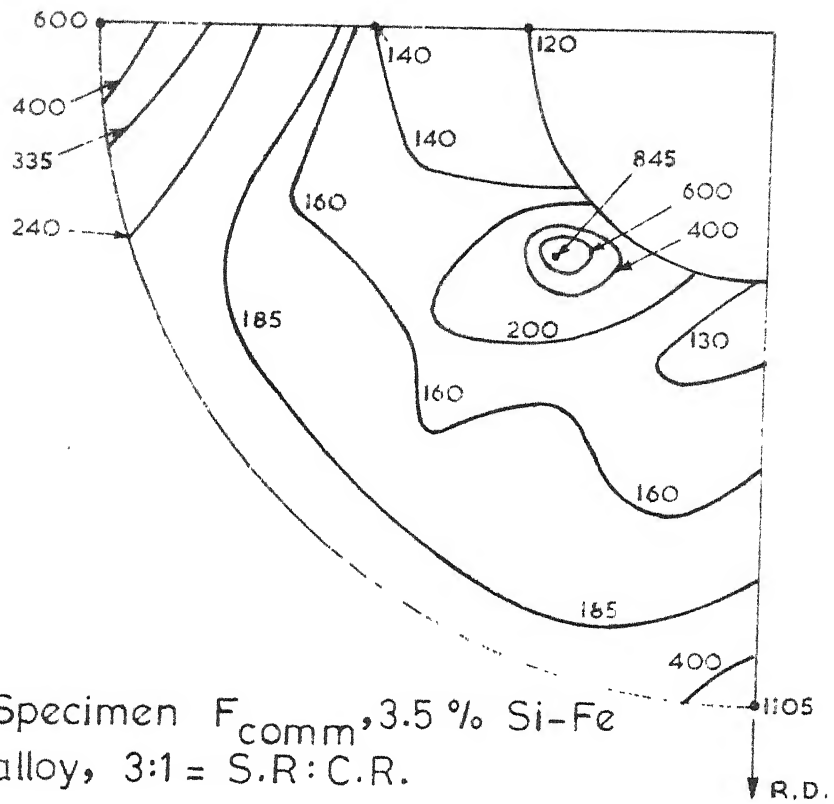
Fig. 43   Specimen F_{comm}, 3.5% Si–Fe alloy, 3:1 = S.R : C.R.
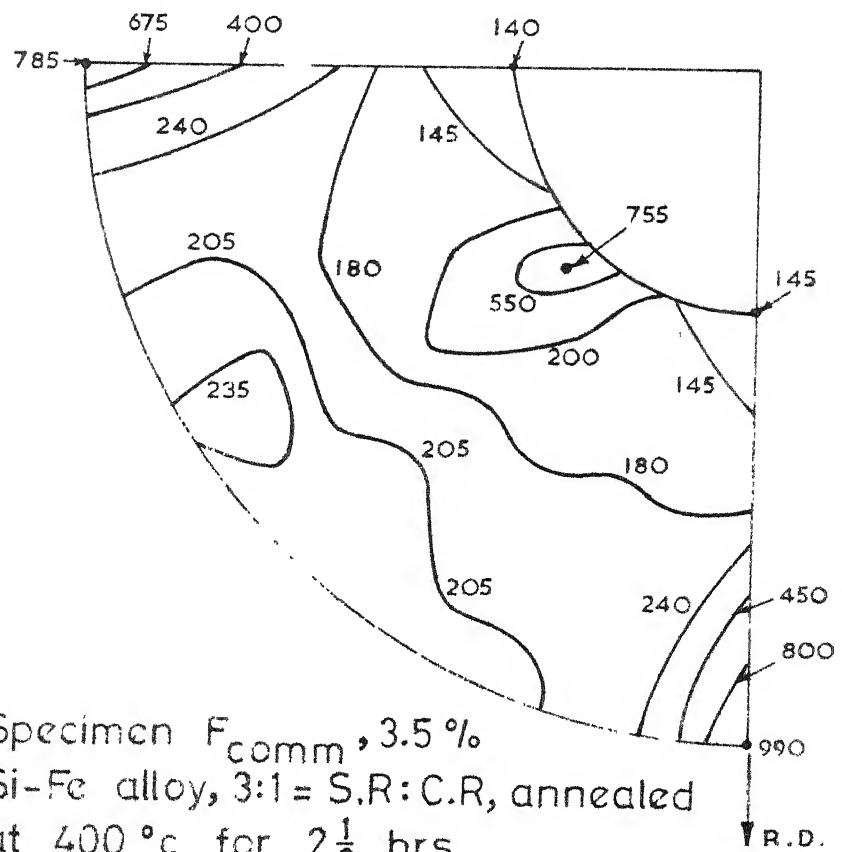
Fig. 44   Specimen F_{comm}, 3.5% Si–Fe alloy, 3:1 = S.R : C.R, annealed at 400°c for $2\frac{1}{2}$ hrs.
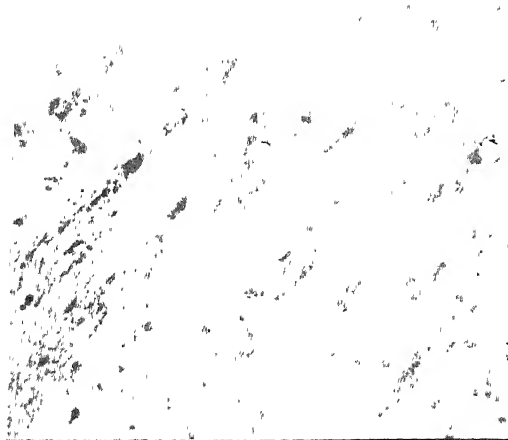
Fig. 45   Pure 3% Si-Fe alloy (G) SR:CR = 3:1;
annealed at 400°C for $2\frac{1}{2}$ hrs 200 x
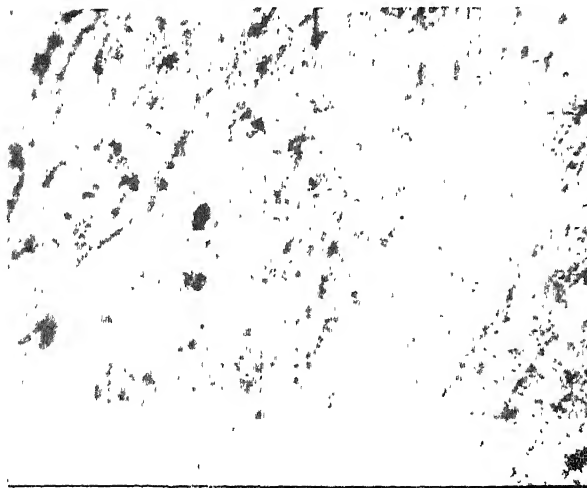
Fig. 46$_a$ Pure 3% Si-Fe alloy (G) SR:CR=3:1;
annealed at 550°C for $\frac{1}{2}$ hr 200 x
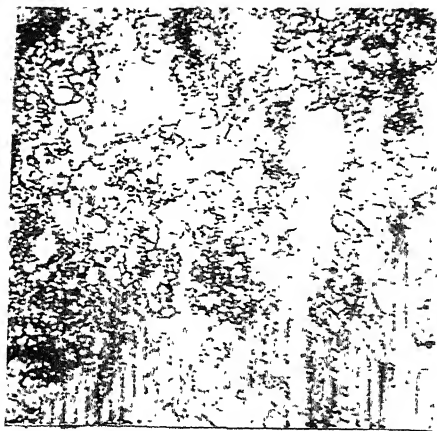
Fig. 47   Pure 3.5% Si-Fe alloy (A) SR:CR=3:1; annealed at 400°C for $2\frac{1}{2}$ hrs 400 x
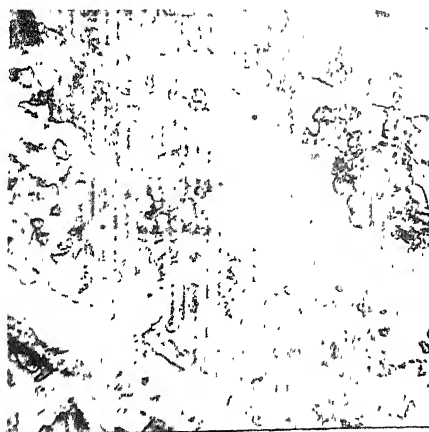
Fig. 46$_b$ Same as Fig. 46$_a$, but at higher magnification (3% Si-Fe alloy; SR:CR=3:1; annealed at 550°C for $\frac{1}{2}$ hr) 400 x
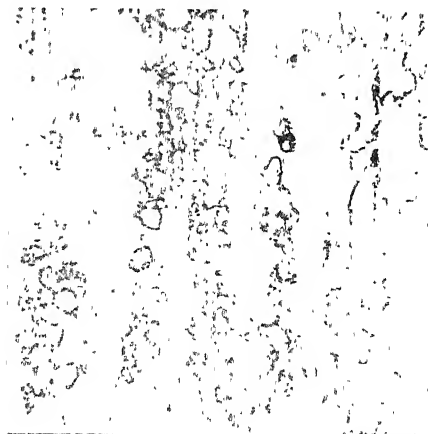
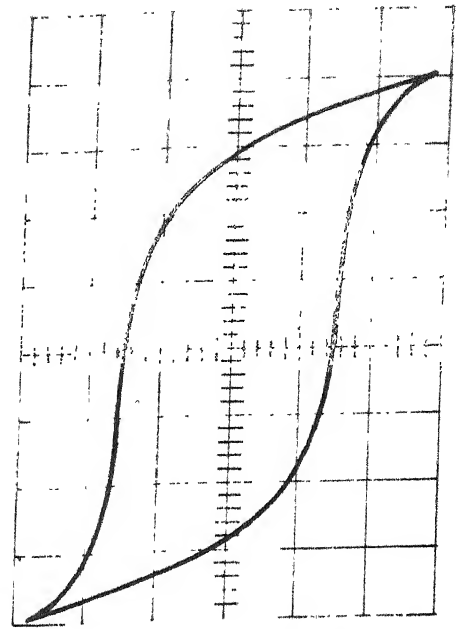Fig. 48   Pure 3.5% Si-Fe alloy (A); SR:CR=3.1; annealed at 550°C for $\frac{1}{2}$ hr   400 x
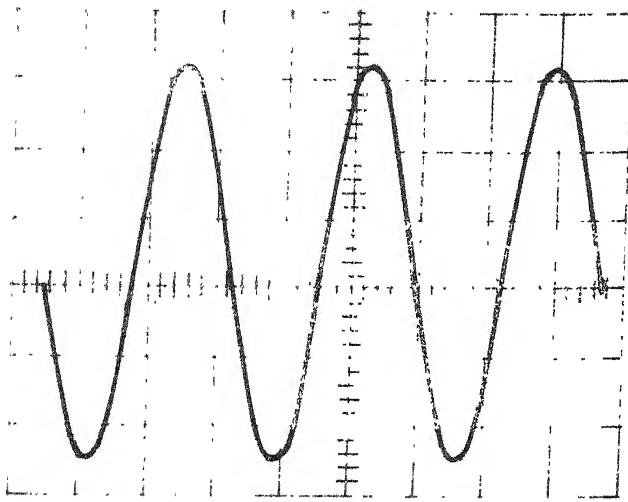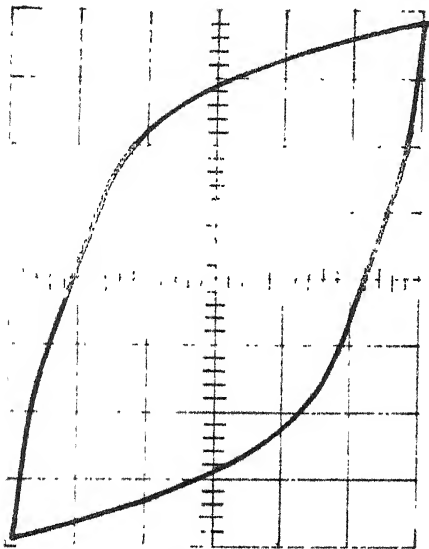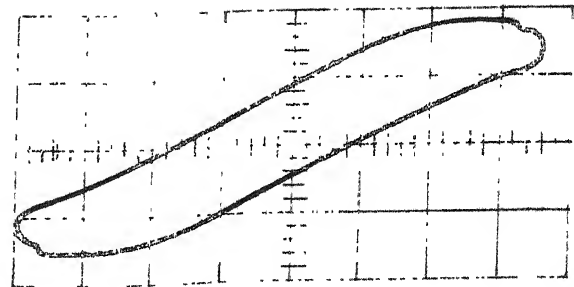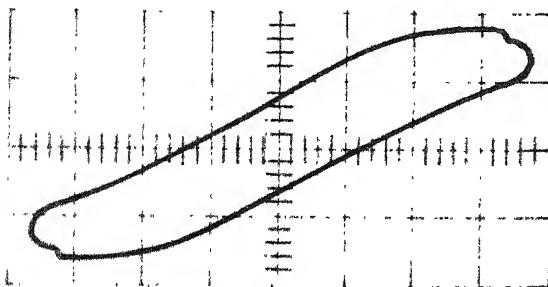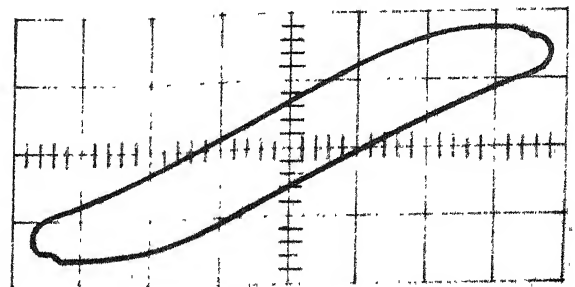
Fig. 49

Fig. 50

Fig. 51

Fig. 52

Fig. 53

Fig. 54

Appendix I

A. Voltage for a given level of flux density

Voltages to be applied across the solenoid terminals so as to obtain the required level of flux density:

$$V = 4.444 \ B \ A \ N_2 F \ 10^{-8} \qquad \dots \qquad (1)$$

where

V = induced secondary voltage (rms), Volts

B = flux density, Gauss

N_2 = number of turns in secondary windings, 700

F = frequency, 50 cps

A = effective cross-sectional area of test specimen, cm^2

$$= \frac{m}{4 \ 1 \ d}$$

where

m = total mass of specimen strips, gm

l = length of strips, 30.5 cm

d = density of specimen material, 7.85 g/cm^3

Appendix II

A. Core loss

To obtain the specific core loss of the specimen in watts per unit mass, it is necessary to subtract all the secondary circuit power included in wattmeter indication before dividing by the "active mass" of the specimen, so that for a specific induction and frequency the specific core loss in watts per unit mass is as follows:

$$\frac{P_c}{m} = \frac{(W - V^2/R)}{m_1} \qquad \dots \qquad (1)$$

where

W = watts indicated by the wattmeter

V = secondary voltage, volts

R = parallel resistance of wattmeter potential
    circuit and all other connected secondary loads, ohms

m_1 = active mass of specimens, kg.

In the 25 cm Epstein frame, it is assumed that 94 cm is the "effective magnetic path" with specimen strips 28 cm or longer. For the purpose of computing core loss, the active mass (less than the actual mass) is assumed to be as follows:

$$m_1 = \frac{94\ m}{4\ l} \qquad \dots \qquad (2)$$

where

m = total specimen mass in desired units, and

l = actual strip length, 30.5 cm

Appendix III

Hysteresis loss

$$W_h = k \cdot \frac{A}{4} \cdot \frac{10^{-4} \cdot f}{d} \qquad \text{watts/kg} \quad \dots \quad (1)$$

where

A = area of the hysteresis loop, cm^2

K = a constant, which is the product of the value
of magnetizing force in o Oersteds per 1 cm of
abscissal and the value of flux density in
Gauss per I cm of ordinate.

f = frequency, cps

d = density of the specimen material, gm/cm^3

ME- 1972-M-KUM-STU